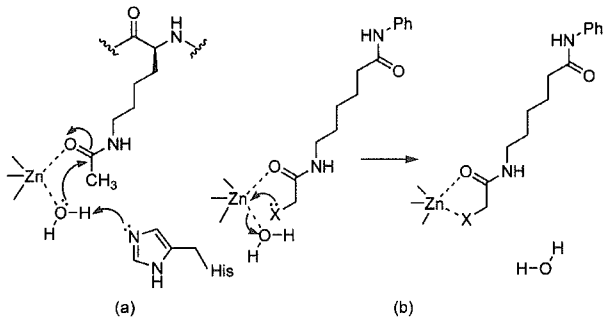

Figure 2. The mechanism proposed for the deacetylation of acetylated lysine substrate (a), and a model for the binding of heteroatom-containing substrate analogues to zinc ion (b).

Table 1. HDAC Inhibition Data for SAHA and SAHA-based Non-hydroxamtes[a]

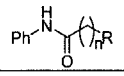

entry	compd	R	*n*	% inhbtn at 100 μM	IC_{50} (μM)
1	SAHA[b]	-CONHOH	6	100	0.28
2	**1**[c]	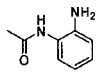	6	48	120
3	**2**	-COCONHMe	6	ND	0.34[d]
4	**3**		7	ND	2.8[e]
5	**4**	-NHCONHOH	5	58	80
6	**5**	-NHCONHNH$_2$	5	35	150
7	**6**	-SO$_2$NHOH	6	14	>100
8	**7**	-SH	6	100	0.21
9	**8a**	-SAc	6	85	7.1
10	**9**	-SMe	6	11	>100
11	**10**	-NHSO$_2$Me	5	10	7500
12	**11**	-SO$_2$Me	6	33	230
13	**12**[f]	-NHCOCH$_2$NH$_2$	5	6	>100
14	**13**	-NHCOCH$_2$OH	5	0	>100
15	**14**	-NHCOCH$_2$SH	5	99	0.39
16	**15**	-NHCOCH$_2$SAc	5	72	22
17	**16**		5	14	>100
18	**17**		5	0	>100
19	**18**	-NHCOCH$_2$Br	5	78	17

[a] Values are means of at least three experiments. [b] Prepared as described in ref 26. [c] Prepared as described in ref 9a. [d] Data taken from the literature (ref 11b). [e] Data taken from the literature (ref 12). [f] Trifluoroacetic acid salt. ND = No data.

Table 2. Effect of Linker Variation on HDAC Inhibitory Activity of Thiols[a]

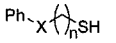

entry	compd	X	*n*	IC_{50} (μM)
1	**7**	-NHCO-	6	0.21
2	**19**	-NHCO-	7	1.5
3	**20**	-NHCO-	5	0.37
4	**21**	-NHCO-	4	6.2
5	**22**	-O-	6	11
6	**23**	-CONH-	6	0.36

[a] Values are means of at least three experiments.

Table 3. Effect of Aromatic Group Variation on HDAC Inhibitory Activity of Thiols[a]

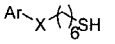

entry	compd	Ar	X	IC_{50} (μM)
1	7	-Ph	-NHCO-	0.21
2	**24**	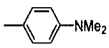	-NHCO-	1.2
3	**25**	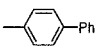	-NHCO-	1.1
4	**26**	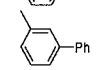	-NHCO-	0.075
5	**27**	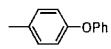	-NHCO-	0.62
6	**28**	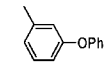	-NHCO-	0.21
7	**29**	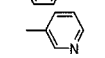	-NHCO-	0.11
8	**30**	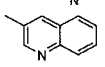	-NHCO-	0.072
9	**31**	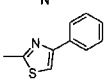	-NHCO-	0.17
10	**32**	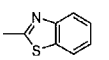	-NHCO-	0.34
11	**23**	-Ph	-CONH-	0.36
12	**33**	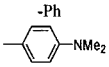	-CONH-	0.61
13	**34**	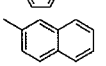	-CONH-	0.085
14	**35**	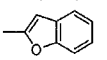	-CONH-	0.079
15	**36**	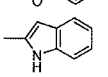	-CONH-	0.10

[a] Values are means of at least three experiments.

With this mechanism, if the water molecule is forcibly removed from the zinc ion, the HDACs would supposedly be inhibited. We then designed and synthesized heteroatom-containing substrate analogues **12**, **13**, and **14**. These analogues would be recognized as substrates by HDACs and would be easily taken into the active site where they could force the water molecule off the zinc ion and the reactive site for the deacetylation by chelation of the heteroatom to the zinc ion, and might behave as HDAC inhibitors (Figure 2b). As shown in Table 1 (entries 13, 14, and 15), potent inhibition was observed with mercaptoacetamide **14**, while **12** and **13** did not possess HDAC inhibitory activities. Mercaptoacetamide **14** exhibited an IC_{50} of 0.39 μM, and its activity largely surpassed those of *o*-aminoanilide **1** and *N*-formyl hydroxylamine **3** and was comparable to those of α-ketoamide **2** and SAHA. As expected, thiol transformation into thioacetate (**15**) led to a 55-fold less potent inhibitor. This result suggests the ease of ionization of thiol is an important factor for HDAC inhibition like the case of thiol **7**.

We turned our attention to irreversible HDAC inhibitors. TPX B is an irreversible HDAC inhibitor,[20] and finding more specific and simpler irreversible HDAC inhibitors is useful for the isolation and cloning of an HDAC.[2] As described above, the crystal structures of the HDLP/hydroxamates and HDAC8/hydroxamates complexes revealed that the hydroxamic acid group forms three hydrogen bonds with Tyr 306, His 143, and His 142, and furthermore, zinc ion is coordinated by His 180, Asp 178, and Asp 267 (HDAC8 numbering). Since the phenol group of Tyr, the imidazole group of His, and the carboxyl group of Asp are able to react with electrophiles, we prepared analogues bearing propargyl

Table 4. Cell Growth Inhibition Data on NCI-H460 Cells for Compound **7** and Its *S*-Modified Prodrugs[a]

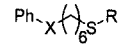

entry	compd	R	EC_{50} (μM)
1	**7**	-H	>50[b]
2	**37**	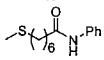	>50[c]
3	**8a**	-Ac	36
4	**38**	-COEt	28
5	**39**	-CO*n*-Pr	22
6	**40**	-CO*i*-Pr	20
7	**41**	-CO*t*-Bu	>50[d]
8	**42**		27
9	**43**		21
10	**44**	-Bz	25
11	**45**	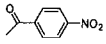	24
12	**46**	-CH_2OCO*t*-Bu	25

[a] Values are means of at least two experiments. [b] 34% inhibition at 50 μM. [c] 10% inhibition at 50 μM. [d] 42% inhibition at 50 μM.

amino (**16**, **17**) and bromoacetamide (**18**) which could form covalent bonds with Tyr, His, and Asp of the enzyme, and evaluated their anti-HDAC activities. While propargyl amino compounds **16** and **17** did not possess HDAC inhibitory activities, more potent inhibition was observed with bromoacetamide **18** (entries 17, 18, and 19). Bromoacetamide **18** exhibited an IC_{50} of 17 μM and its activity was about 9-fold as strong as that of *o*-aminoanilide **1**, but much weaker than that of SAHA.

With the results shown in Table 1, we were encouraged to study further the structure–activity relationship (SAR) and structural optimization. We selected thiol **7** for further study.[21] First, we examined the effect of linker parts of thiol **7**. The results are summarized in Table 2. HDAC inhibition was distinctly dependent on chain length, with $n = 7$ (**19**) and $n = 4$ (**21**) resulting in less potent inhibitors. However, compound **20**, in which $n = 5$, showed essentially the same potency as compound **7**, in which $n = 6$ (entries 1–4). The similar SAR between thiols and hydroxamates, with $n = 6$ optimal,[22] indicates that thiols inhibit HDACs in a binding mode similar to that of hydroxamates. As for the group attaching the phenyl moiety, ether **22** displayed moderate activity, whereas the activity of the reversed amide **23** was maintained (entries 5 and 6).

Next, the aromatic group was examined (Table 3). In the amide-linked series (entries 1–10), 4-substituted phenyl compounds tended to decrease the potency. Specifically, compounds **24** (Ar = 4-NMe_2-Ph), **25** (Ar = 4-biphenyl), and **27** (Ar = 4-PhO-Ph) showed about a 3- to 6-fold decrease in potency when compared to the parent thiol **7** (entries 2, 3, and 5). On the other hand, compound **26**, in which a phenyl group was introduced at the 3-position of the phenyl group of **7**, showed 3-fold increased inhibitory activity (IC_{50} of 0.075 μM, entry 4). In addition, 3-phenoxy compound **28** was equipotent with compound **7** (entry 6). We investigated the effect of the replacement of the phenyl group of compound **7** with heteroaryl rings (entries 7, 8, 9, and 10). Changing the benzene ring to a 3-pyridine ring (**29**), 4-phenyl-2-thiazole ring (**31**), and 2-benzothiazole ring (**32**) sustained or slightly reduced the activity, whereas quinoline **30** had improved activity (IC_{50} of 0.072 μM), and turned out to be the most potent compound in this series. The reverse amide-linked series (entries 11–15) exhibited potencies similar to or greater than the parent thiol **23**, with the exception of **33** (Ar = 4-NMe_2-Ph), which resulted in a slightly less potent inhibitor. In particular, the reversed amides **34** with a naphthalene substituent and **35** with a benzofuran substituent exhibited about 3-fold increases in potency (IC_{50}s of 0.085 μM and 0.079 μM, respectively). As a result, IC_{50}s in the double-digit nanomolar range were observed with 3-biphenyl **26**, quinoline **30**, naphthalene **34**, and benzofuran **35**, which were approximately 3- to 4-fold more potent than SAHA.

Table 5. Cell Growth Inhibition Data on NCI-H460 Cells for Compound **40** and Its Derivatives[a]

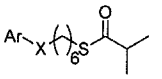

entry	compd	Ar	X	EC_{50} (μM)
1	**40**	-Ph	-NHCO-	20
2	**47**		-NHCO-	2.8
3	**48**		-NHCO-	25
4	**49**		-NHCO-	2.9
5	**50**		-NHCO-	8.0
6	**51**		-NHCO-	2.1
7	**52**		-NHCO-	9.5
8	**53**		-CONH-	12
9	**54**		-CONH-	4.1
10	**55**		-CONH-	12

[a] Values are means of at least two experiments.

Table 6. Growth Inhibition of Various Cancer Cells Using SAHA and Compound **51**[a]

	cell	SAHA, EC_{50} (μM)	**51**, EC_{50} (μM)
MDA-MB-231	breast cancer	1.5	2.3
SNB-78	central nervous system	16	9.1
HCT116	colon cancer	0.58	3.0
NCI–H226	lung cancer	2.6	2.6
LOX-IMVI	melanoma	1.3	1.1
SK-OV-3	ovarian cancer	2.5	4.5
RXF-631L	renal cancer	2.0	2.4
St-4	stomach cancer	5.2	5.0
DU-145	prostate cancer	1.6	4.5
	mean	3.7	3.8

[a] Values are means of at least two experiments.

Cancer Cell Growth Inhibition Assay. To confirm the effectiveness of thiol-based HDAC inhibitors as anticancer drugs and tools for biological research, thiol **7** was initially tested in a cancer cell growth inhibition

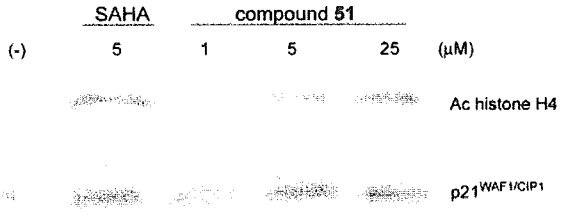

Figure 3. Western blot analysis of histone hyperacetylation and $p21^{WAF1/CIP1}$ induction in HCT 116 cells produced by compound **51** and by reference compound SAHA.

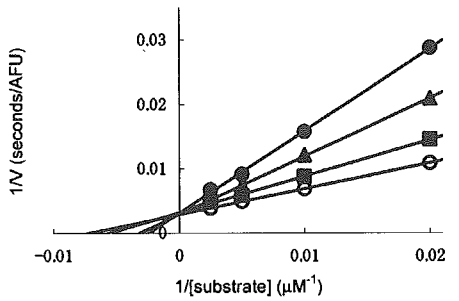

Figure 4. Reciprocal rate vs reciprocal acetylated lysine substrate concentration in the presence of 0.3 (●), 0.1 (▲), 0.03 (■), and 0 (○) μM of **7**.

assay using human lung cancer NCI-H460 cells against which it was found to be only weakly potent, although **7** was highly active in an enzymatic assay (Table 4, entry 1). The reason for the weak activity of thiol **7** is unclear, but it is reasonable to assume that it was due to poor membrane permeability resulting from the highly polar character of this compound, and that a transient masking of the sulfhydryl group could improve its permeability and its ability to inhibit cancer cell growth. Therefore, we investigated the possibility of improving the inhibition using the prodrug approach. In the search for a suitable prodrug of thiols, disulfides seemed to be attractive targets, because it has been reported that the disulfide bond of macrocyclic compounds bearing a disulfide group such as FK228 is reduced in the cellular environment, releasing the free thiol analogue as the active species.[17] However, contrary to our expectation, disulfide **37** failed to exhibit a growth inhibitory effect on NCI-H460 cells (entry 2). Next, we examined the activity of acetyl compound **8a**. Acetyl compound **8a** proved to be relatively potent compared with thiol **7** and disulfide **37** (EC_{50} of 36 μM) (entry 3). This result suggests that **8a** permeates the cell membrane more efficiently than thiol **7**, and is converted to thiol **7** by enzymatic hydrolysis within the cell.[23] Encouraged by this finding, we prepared other *S*-acyl compounds (**38**–**45**) and evaluated their activities (entries 4–11). This series of compounds exhibited greater potency than acetyl compound **8a**, except for pivaloyl compound **41**, which was a less potent inhibitor. In particular, isobutyryl compound **40** showed about a 2-fold increase in activity when compared to acetyl compound **8a** (EC_{50} of 20 μM). The compound bearing a (pivaloyloxy)methyl group[24] (**46**) was slightly less active than isobutyryl compound **40** (entry 12).

With the results shown in Table 4, a selected set of active compounds from the enzymatic assay was *S*-isobutyrylated and tested as cancer cell growth inhibitors (Table 5). Much to our satisfaction, changing the phenyl group of compound **40** to other aromatic groups led to positive results. Isobutyryl analogues **47**–**55** were generally more potent than the parent compound **40**; the sole exception is **48** (Ar = 3-OPh-Ph) which was slightly less active than compound **40** (entry 3). Notably, 3-biphenyl (**47**), 3-pyridinyl (**49**), and 4-phenyl-2-thiazolyl (**51**) analogues showed strong activity in inhibiting the growth of NCI-H460 cells, with EC_{50}s of 2–3 μM. Furthermore, we evaluated cancer cell growth inhibition by SAHA and **51**, the most potent compound in this study, against nine other human cancer cell lines

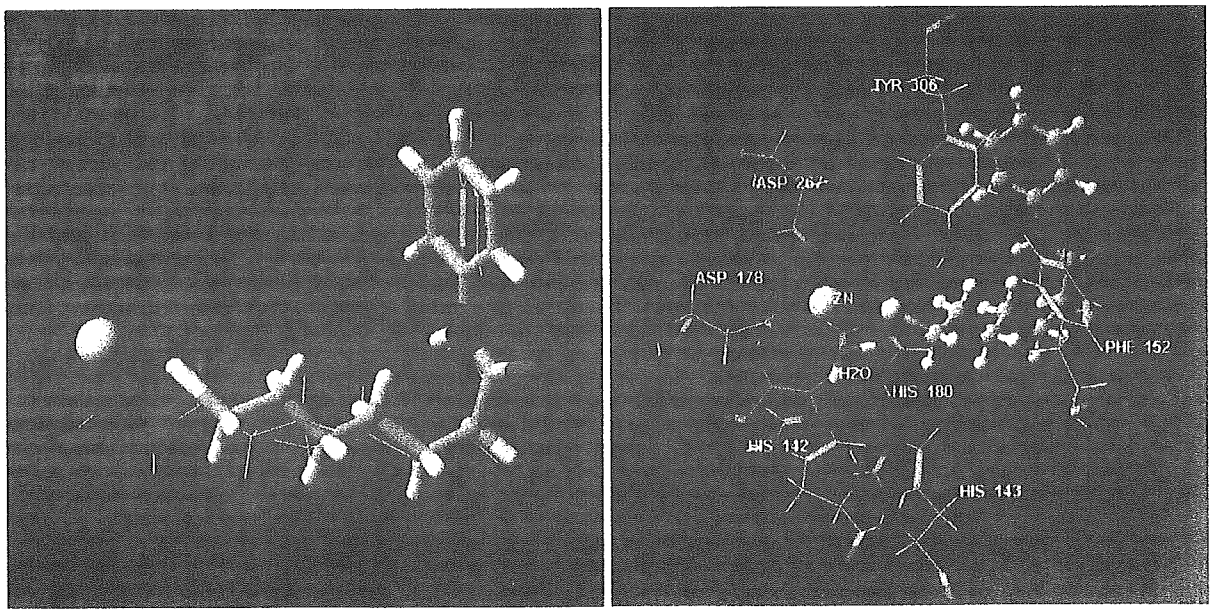

Figure 5. Superposition of the low energy conformations of **7** (tube) and SAHA (wire) (left). The HDAC8 pocket is not shown for the sake of clarity. View of the conformation of **7** (ball-and-stick) docked in the HDAC8 catalytic core (right). Residues around the zinc ion and a water molecule are displayed as wires and tubes, respectively.

(Table 6). Compound **51** exerted potent growth inhibition against various human cancer cells, with EC_{50} values ranging from 1 to 10 μM, and these inhibitory activities were comparable to those of SAHA (average EC_{50} of **51** 3.8 μM, SAHA 3.7 μM) which is currently being evaluated in clinical trials for use in the treatment of cancer.

By Western blot analysis, cancer cell growth inhibition with compound **51** was verified to be the result of inhibition of HDACs (Figure 3). Treatment of HCT 116 cells with compound **51** gave rise to elevated and dose-dependent levels of acetylated histone H4 and $p21^{WAF1/CIP1}$.

Inhibitory Mechanism Study. Since the results of cancer cell growth inhibition and Western blot analysis have suggested that thiols generated from *S*-acyl prodrugs by enzymatic hydrolysis within the cell inhibit intracellular HDACs, we next studied the mechanism by which thiols inhibit HDACs in greater detail. Although the sulfhydryl group of thiol derivatives was designed as a ZBG, it is possible that thiols inhibit HDACs by forming a covalent disulfide bond with cysteine residues on these enzymes. We examined this possibility using a double reciprocal plot of 1/V versus 1/[substrate] at varying concentrations of inhibitor **7** (Figure 4), and the data from this study established that thiol **7** engages in competitive inhibition versus acetylated lysine substrate, with an inhibition constant (K_i) of 0.11 μM. Since cysteine is not a component in the construction of the active site of HDACs, the sulfhydryl group of **7** likely interacts with the zinc in the active site.

Binding Mode Study. Since thiol **7** proved to be a competitive inhibitor and to act within the active center of HDACs, we studied its binding mode within this site. The low energy conformations of **7** and SAHA were calculated when docked in the model based on the crystal structure of HDAC8 (PDB code 1T64, 1T67, 1T69, and 1VKG) using Macromodel 8.1 software.[25] The anilide group and alkyl chain of **7** and SAHA were essentially superimposed in the binding pocket, and the binding mode of **7** was found to be similar to that of SAHA (Figure 5, left). An inspection of the HDAC8/**7** complex shows that the sulfur atom of **7** was located 2.35 Å from the zinc ion, 2.24 Å from the OH group of Tyr 306, and 2.66 Å from a water molecule which forms a hydrogen bond with the imidazole group of His142 (Figure 5, right). This suggests that thiols strongly inhibit HDACs by interacting directly with zinc ion, Tyr 306, and His 142 via a water molecule.

Conclusion

We have designed and prepared a series of SAHA-based compounds as (i) hydroxamic acid mimics by structure-based drug design (compounds **4**–**6**), (ii) thiol-based analogues (compounds **7**–**9**), (iii) transition-state analogues (compounds **10** and **11**), (iv) heteroatom-containing substrate analogues by mechanism-based drug design (compounds **12**–**15**), and (v) irreversible inhibition-oriented compounds (compounds **16**–**18**), and evaluated their inhibitory effect on HDACs. In this series, thiol **7** and mercaptoacetamide **14** were found to be much more potent HDAC inhibitors than previously reported non-hydroxamates, and as potent as α-ketoamide **2** and SAHA. At present, thiol is one of the most active ZBG among small-molecule HDAC inhibitors. Optimization of thiol derivatives led to the identification of inhibitors more effective than SAHA (compounds **26**, **30**, **34**, and **35**). We have also identified a potent cancer cell growth inhibitor, compound **51**, by the prodrug formation of thiol-based HDAC inhibitors. Thiol **7** exhibits strong competitive inhibition of an acetylated lysine substrate, and molecular modeling suggests that the thiol interacts with zinc, Tyr 306, and His 142 (HDAC8 numbering) in the active site.

In conclusion, we have identified several new lead structures including thiol, from which more potent HDAC inhibitors can be developed. As far as we could determine, this is the first systematic study of ZBGs for HDAC inhibitors. We believe that the findings of this study should be of value in future studies for the development of ideal anticancer drugs and tools for biological research such as HDAC isozyme-selective inhibitors.

Experimental Section

Chemistry. Melting points were determined using a Yanagimoto micro melting point apparatus or a Büchi 545 melting point apparatus and were left uncorrected. Proton nuclear magnetic resonance spectra (^{1}H NMR) were recorded on a JEOL JNM-LA400 or JEOL JNM-LA500 spectrometer in solvent as indicated. Chemical shifts (δ) are reported in parts per million relative to the internal standard tetramethylsilane. Elemental analysis was performed with a Yanaco CHN CORDER NT-5 analyzer, and all values were within ±0.4% of the calculated values. High-resolution mass spectra (HRMS) were recorded on a JEOL JMS−SX102A mass spectrometer. GC-MS analyses were performed on a Shimadzu GCMS-QP2010. Reagents and solvents were purchased from Aldrich, Tokyo Kasei Kogyo, Wako Pure Chemical Industries, and Kanto Kagaku and used without purification. Flash column chromatography was performed using silica gel 60 (particle size 0.046−0.063 mm) supplied by Merck.

6-(3-Hydroxyureido)hexanoic Acid Phenylamide (4). Step 1: Preparation of 6-Phenylcarbamoylhexanoic Acid (57). A mixture of aniline (5.80 g, 62.3 mmol) and pimeric acid (**56**, 10.0 g, 62.4 mmol) was stirred at 180 °C for 1 h. After cooling, the mixture was diluted with AcOEt-THF and the slurry was filtered. The filtrate was washed with saturated aqueous $NaHCO_3$, and the aqueous layer was acidified with concentrated HCl. The precipitated crystals were collected by filtration to give 7.11 g (49%) of **57** as a white solid: ^{1}H NMR (DMSO-d_6, 400 MHz, δ; ppm) 11.97 (1H, broad s), 9.83 (1H, s), 7.58 (2H, d, J = 7.8 Hz), 7.27 (2H, t, J = 7.9 Hz), 7.01 (1H, t, J = 7.4 Hz), 2.67 (2H, t, J = 7.4 Hz), 2.21 (2H, t, J = 7.3 Hz), 1.62−1.49 (4H, m), 1.34−1.27 (2H, m).

Steps 2 and 3: Preparation of 6-(3-Hydroxyureido)-hexanoic Acid Phenylamide (4). To a suspension of **57** (958 mg, 4.07 mmol) obtained above and triethylamine (744 mg, 7.35 mmol) in toluene (10 mL) was added diphenylphosphoryl azide (1.75 g, 6.34 mmol), and the mixture was heated at reflux temperature for 1h. Next, *O*-(2-tetrahydropyranyl)hydroxylamine (380 mg, 3.11 mmol) was added, and the reaction mixture was stirred at reflux temperature for 18h. It was then concentrated in vacuo, and the residue was dissolved in AcOEt. The AcOEt solution was washed with water, saturated aqueous $NaHCO_3$, and brine and was dried over Na_2SO_4. Filtration and concentration in vacuo and purification by silica gel flash chromatography (*n*-hexane/AcOEt = 1/2) gave 988 mg (69%) of the *O*-(2-tetrahydropyranyl)hydroxyurea as a white solid: ^{1}H NMR ($CDCl_3$, 500 MHz, δ; ppm) 7.53 (2H, d, J = 7.9 Hz), 7.32 (2H, t, J = 7.8 Hz), 7.26 (1H, broad s), 7.10 (1H, t, J = 7 Hz), 7.05 (1H, broad s), 6.06 (1H, broad s), 4.75 (1H, d, J = 3.6 Hz), 3.93 (1H, m), 3.57 (1H, m), 3.33−3.26 (2H, m), 2.38 (2H, t, J = 7.5 Hz), 1.82−1.77 (4H, m), 1.61−1.55 (6H, m), 1.44 (2H, quintet, J = 7.3 Hz).

To a solution of the *O*-(2-tetrahydropyranyl)hydroxyurea (185 mg, 0.53 mmol) obtained above in MeOH (2 mL) was added 4-toluenesulfonic acid monohydrate (15 mg, 0.079 mmol). The solution was stirred overnight at room temperature, and the precipitated crystals were collected by filtration to give 46 mg (32%) of **4** as a white solid. The solid was recrystallized from MeOH–AcOEt and collected by filtration to give 34 mg of **4** as a colorless crystal: mp 148–149 °C; ^{1}H NMR (DMSO-d_6, 500 MHz, δ; ppm) 9.93 (1H, s), 8.58 (1H, s), 8.29 (1H, s), 7.65 (2H, d, J = 8 Hz), 7.35 (2H, t, J = 7.9 Hz), 7.08 (1H, t, J = 7.3 Hz), 6.75 (1H, t, J = 6 Hz), 3.10 (2H, q, J = 6.7 Hz), 2.36 (2H, t, J = 7.5 Hz), 1.65 (2H, quintet, J = 7.5 Hz), 1.50 (2H, quintet, J = 7.2 Hz), 1.34 (2H, quintet, J = 7.6 Hz); Anal. ($C_{13}H_{19}N_3O_3$) C, H, N.

6-(3-Aminoureido)hexanoic Acid Phenylamide (5). Compound **5** was prepared from **57** obtained above by using the procedure described for **4** (step 2) in 52% yield. In this case, hydrazine monohydrate was used instead of *O*-(2-tetrahydropyranyl)hydroxylamine: mp 146–147 °C; ^{1}H NMR (DMSO-d_6, 400 MHz, δ; ppm) 9.83 (1H, s), 7.58 (2H, d, J = 7.8 Hz), 7.27 (2H, t, J = 7.9 Hz), 7.01 (1H, t, J = 7.3 Hz), 6.83 (1H, broad s), 6.28 (1H, broad s), 4.03 (2H, broad s), 3.01 (2H, q, J = 6.7 Hz), 2.29 (2H, t, J = 7.4 Hz), 1.60–1.57 (2H, m), 1.40–1.38 (2H, m), 1.32–1.28 (2H, m); MS (EI) *m/z*: 264 (M^+); Anal. ($C_{13}H_{20}N_4O_2$) C, H, N.

6-Methanesulfonylaminohexanoic Acid Phenylamide (10). Steps 1 and 2: Preparation of 6-Aminohexanoic Acid Phenylamide (58). To a suspension of **57** (1.11 g, 4.73 mmol) obtained above and triethylamine (699 mg, 6.90 mmol) in benzene (3 mL) was added diphenylphosphoryl azide (1.83 g, 6.64 mmol), and the mixture was heated at reflux temperature for 1 h. Next, benzyl alcohol (1.20 mL, 11.6 mmol) was added, and the reaction mixture was stirred at reflux temperature for 24 h. It was then concentrated in vacuo and the residue was dissolved in AcOEt. The AcOEt solution was washed with 0.4 N aqueous HCl, water, saturated aqueous $NaHCO_3$, and brine and was dried over Na_2SO_4. Filtration and concentration in vacuo and purification by recrystallization from $CHCl_3$–*n*-hexane gave 1.01 g (63%) of (6-phenylcarbamoylpentyl)carbamic acid benzyl ester as a colorless needle: ^{1}H NMR (DMSO-d_6, 400 MHz, δ; ppm) 9.81 (1H, s), 7.57 (2H, d, J = 7.8 Hz), 7.37–7.22 (8H, m), 7.00 (1H, t, J = 7.4 Hz), 4.99 (2H, s), 2.99 (2H, q, J = 6.5 Hz), 2.28 (2H, t, J = 7.4 Hz), 1.58 (2H, quintet, J = 7.6 Hz), 1.43 (2H, quintet, J = 7.1 Hz), 1.32 (2H, quintet, J = 7.8 Hz); MS (EI) *m/z*: 340 (M^+).

A solution of (6-phenylcarbamoylpentyl)carbamic acid benzyl ester (1.00 g, 2.95 mmol) obtained above in MeOH (50 mL) was stirred under H_2 (atmospheric pressure) in the presence of 5% Pd/C (106 mg) at room temperature for 7 h. The catalyst was removed by filtration through Celite, and the filtrate was concentrated in vacuo. The residue was purified by silica gel flash chromatography ($CHCl_3$/MeOH/*i*PrNH$_2$ = 19/1/1) to give 584 mg (96%) of **58** as a white solid: ^{1}H NMR (DMSO-d_6, 400 MHz, δ; ppm) 9.83 (1H, s), 7.58 (2H, d, J = 7.6 Hz), 7.27 (2H, t, J = 7.9 Hz), 7.01 (1H, t, J = 7.3 Hz), 2.55 (2H, m), 2.29 (2H, t, J = 7.4 Hz), 1.59 (2H, quintet, J = 7.4 Hz), 1.37–1.30 (4H, m).

Step 3: Preparation of 6-Methanesulfonylaminohexanoic Acid Phenylamide (10). To a solution of **58** (500 mg, 2.06 mmol) obtained above in pyridine (5 mL) was added methanesulfonyl chloride (160 μL, 2.07 mmol) dropwise with cooling in an ice–water bath. The solution was stirred for 30 min at room temperature. The mixture was concentrated and diluted with AcOEt. The solution was washed with 2 N aqueous HCl, water, and brine and was dried over Na_2SO_4. Filtration and concentration in vacuo and purification by silica gel flash chromatography (*n*-hexane/AcOEt = 1/3) gave 418 mg (71%) of **10** as a crude solid. The solid was recrystallized from AcOEt to give **10** (214 mg) as colorless crystals: mp 136–137 °C; ^{1}H NMR (DMSO-d_6, 500 MHz, δ; ppm) 9.85 (1H, s), 7.58 (2H, d, J = 7.7 Hz), 7.28 (2H, t, J = 7.4 Hz), 7.01 (1H, t, J = 7.4 Hz), 6.93 (1H, t, J = 6.5 Hz), 2.92 (2H, q, J = 6.5 Hz), 2.87 (3H, s), 2.30 (2H, t, J = 7.6 Hz), 1.59 (2H, quintet, J = 7.6 Hz), 1.59 (2H, quintet, J = 7.6 Hz), 1.48 (2H, quintet, J = 7.4 Hz), 1.33 (2H, quintet, J = 7.4 Hz); MS (EI) *m/z*: 284 (M^+); Anal. ($C_{13}H_{20}N_2O_3S$) C, H, N.

6-(2-Hydroxyacetylamino)hexanoic Acid Phenylamide (13). To a solution of **58** (198 mg, 0.96 mmol) and glycolic acid (81 mg, 1.07 mmol) in DMF (6 mL) were added 1-ethyl-3-(3-dimethylaminopropyl)carbodiimide hydrochloride (254 mg, 1.32 mmol) and 1-hydroxy-1*H*-benzotriazole monohydrate (244 mg, 1.59 mmol), and the mixture was stirred overnight at room temperature. The reaction mixture was poured into water and extracted with AcOEt. The AcOEt layer was separated, washed with saturated aqueous $NaHCO_3$ and brine, and dried over Na_2SO_4. Filtration and concentration in vacuo gave 251 mg (99%) of **13** as a crude solid. The solid was recrystallized from AcOEt to give 155 mg of **13** as a colorless crystal: mp 109–113 °C; ^{1}H NMR (DMSO-d_6, 500 MHz, δ; ppm) 9.92 (1H, s), 7.79 (1H, broad s), 7.65 (2H, d, J = 7.6 Hz), 7.35 (2H, t, J = 7.9 Hz), 7.08 (1H, t, J = 7.3 Hz), 5.51 (1H, t, J = 5.8 Hz), 3.84 (2H, d, J = 5.8 Hz), 3.16 (2H, q, J = 6.8 Hz), 2.36 (2H, t, J = 7.5 Hz), 1.65 (2H, quintet, J = 7.5 Hz), 1.51 (2H, quintet, J = 7.3 Hz), 1.35 (2H, quintet, J = 7.9 Hz); MS (EI) *m/z*: 264 (M^+); Anal. ($C_{14}H_{20}N_2O_3$) C, H, N.

6-(2-Aminoacetylamino)hexanoic Acid Phenylamide Trifluoroacetic Acid Salt (12·TFA). Step 1: Preparation of [(5-Phenylcarbamoylpentylcarbamoyl)methyl]carbamic Acid *tert*-Butyl Ester. This compound was prepared from **58** and *N*-(*tert*-butoxycarbonyl)glycine using the procedure described for **13** in 70% yield: ^{1}H NMR ($CDCl_3$, 400 MHz, δ; ppm) 7.53 (2H, d, J = 7.8 Hz), 7.34 (2H, t, J = 7.6 Hz), 7.10 (1H, t, J = 7.6 Hz), 6.14 (1H, broad s), 5.07 (1H, broad s), 3.75 (2H, d, J = 6 Hz), 3.30 (2H, q, J = 6.5 Hz), 2.37 (2H, t, J = 7.4 Hz), 1.76 (2H, quintet, J = 7.4 Hz), 1.58–1.26 (13H, m).

Step 2: Preparation of 6-(2-Aminoacetylamino)hexanoic Acid Phenylamide Trifluoroacetic Acid Salt (12·TFA). To a solution of [(5-phenylcarbamoylpentylcarbamoyl)-methyl]carbamic acid *tert*-butyl ester (147 mg, 0.40 mmol) obtained above in $CHCl_3$ (4 mL) was added trifluoroacetic acid (1 mL), and the mixture was stirred overnight at room temperature. The reaction mixture was concentrated in vacuo, and the residue was triturated in diethyl ether to give 131 mg (84%) of **12**·TFA as a white solid. The solid was recrystallized from AcOEt–MeOH to give 120 mg of **12**·TFA as colorless crystals: mp 149–151 °C; ^{1}H NMR (DMSO-d_6, 500 MHz, δ; ppm) 10.00 (1H, s), 8.43 (1H, t, J = 5.2 Hz), 8.10 (3H, broad s), 7.71 (2H, d, J = 8.2 Hz), 7.41 (2H, t, J = 7.9 Hz), 7.14 (1H, t, J = 7.3 Hz), 3.25 (2H, q, J = 6.4 Hz), 2.43 (2H, t, J = 7.3 Hz), 1.72 (2H, quintet, J = 7.5 Hz), 1.58 (2H, quintet, J = 7.2 Hz), 1.44 (2H, quintet, J = 7.5 Hz); Anal. ($C_{14}H_{21}N_3O_2$·TFA·1/10H_2O) C, H, N.

6-(2-Bromoacetylamino)hexanoic Acid Phenylamide (18). To a solution of **58** (70 mg, 0.340 mmol) and triethylamine (0.40 mL, 2.88 mmol) in THF (2 mL) was added a solution of bromoacetyl bromide (319 mg, 1.58 mmol) in THF (1 mL) dropwise with cooling in an ice–water bath. The mixture was stirred at room temperature for 30 min. The reaction mixture was diluted with $CHCl_3$, washed with aqueous saturated $NaHCO_3$, water, and brine, and dried over Na_2SO_4. Filtration and concentration in vacuo and purification by silica gel flash chromatography ($CHCl_3$/MeOH = 150/1) gave 25 mg (23%) of **18** as a white solid: ^{1}H NMR ($CDCl_3$, 400 MHz, δ; ppm) 7.52 (2H, d, J = 8.1 Hz), 7.32 (2H, t, J = 7.9 Hz), 7.19 (1H, broad s), 7.10 (1H, t, J = 7.6 Hz), 6.56 (1H, broad s), 3.87 (2H, s), 3.32 (2H, q, J = 6.6 Hz), 2.38 (2H, t, J = 7.3 Hz), 1.80–1.76 (2H, m), 1.63–1.59 (2H, m), 1.46–1.44 (2H, m); MS (EI) *m/z*: 326 (M^+); Anal. ($C_{14}H_{19}BrN_2O_2$) C, H, N.

Thioacetic acid *S*-[(6-Phenylcarbamoylpentylcarbamoyl)methyl] Ester (15). To a suspension of **18** (187 mg, 0.57 mmol) obtained above in EtOH (2 mL) was added potassium thioacetate (236 mg, 2.07 mmol), and the mixture was stirred at room temperature for 16 h. The reaction mixture was diluted with AcOEt and THF, washed with water and brine, and dried over Na_2SO_4. Filtration and concentration in vacuo and purification by silica gel flash chromatography (*n*-hexane/AcOEt = 1/1) gave 163 mg (89%) of **15** as a white solid. The solid was recrystallized from *n*-hexane–AcOEt to give 48 mg

of **15** as a colorless crystal: mp 130–133 °C; ^{1}H NMR ($CDCl_3$, 400 MHz, δ; ppm) 7.53 (2H, d, J = 7.3 Hz), 7.32 (2H, t, J = 7.9 Hz), 7.25 (1H, broad s), 7.10 (1H, t, J = 7.2 Hz), 6.25 (1H, broad s), 3.51 (2H, s), 3.25 (2H, q, J = 6.6 Hz), 2.39 (3H, s), 2.37 (2H, t, J = 7.4 Hz), 1.75 (2H, quintet, J = 7.6 Hz), 1.55 (2H, quintet, J = 7.1 Hz), 1.39 (2H, quintet, J = 7.3 Hz); MS (EI) *m/z*: 322 (M^+); Anal. ($C_{16}H_{22}N_2O_3S$) C, H, N.

6-(2-Mercaptoacetylamino)hexanoic Acid Phenylamide (14). To a solution of **15** (190 mg, 0.59 mmol) obtained above in MeOH (5 mL) was added K_2CO_3 (141 mg, 1.02 mmol), and the mixture was stirred at room temperature for 1 h. The reaction mixture was diluted with AcOEt and THF, washed with water and brine, and dried over Na_2SO_4. Filtration and concentration in vacuo and purification by silica gel flash chromatography ($CHCl_3$/MeOH = 20/1) gave 103 mg (62%) of **14** as a white solid. The solid was recrystallized from $CHCl_3$–MeOH to give 38 mg of **14** as a colorless crystal: mp 171–173 °C; ^{1}H NMR (DMSO-d_6, 500 MHz, δ; ppm) 9.84 (1H, s), 8.08 (1H, broad s), 7.57 (2H, d, J = 8.2 Hz), 7.27 (2H, t, J = 7.9 Hz), 7.00 (1H, t, J = 7.3 Hz), 3.90 (1H, s), 3.44 (2H, s), 3.07 (2H, q, J = 6.5 Hz), 2.28 (2H, t, J = 7.5 Hz), 1.59 (2H, quintet, J = 7.3 Hz), 1.45 (2H, quintet, J = 7 Hz), 1.31 (2H, quintet, J = 7.5 Hz); MS (EI) *m/z*: 280 (M^+); Anal. ($C_{14}H_{20}N_2O_2S$) C, H, N.

6-(2-Propynylamino)hexanoic Acid Phenylamide Hydrochloride Salt (16·HCl) and 6-(2-Dipropynylamino)-hexanoic Acid Phenylamide (17). To a solution of **58** (230 mg, 1.12 mmol) obtained above and K_2CO_3 (39 mg, 0.28 mmol) in MeOH (1 mL) was added propargyl bromide (38 mg, 0.32 mmol), and the mixture was stirred overnight at room temperature. The reaction mixture was concentrated in vacuo, and the residue was purified by silica gel flash chromatography ($CHCl_3$/MeOH = 15/1) to give 40 mg (51%) of **16** as a pale yellow oil and 12 mg (23%) of **17** as a pale yellow solid. To a solution of **16** in MeOH was added 1 N aqueous HCl (0.5 mL), and the solution was concentrated in vacuo. The residue was recrystallized from MeOH–AcOEt to give 16 mg of **16**·HCl as colorless needles: mp 161–165 °C; ^{1}H NMR (DMSO-d_6, 400 MHz, δ; ppm) 9.91 (1H, broad s), 9.12 (2H, broad s), 7.59 (2H, d, J = 7.6 Hz), 7.28 (2H, t, J = 7.9 Hz), 7.01 (1H, t, J = 7.3 Hz), 3.89 (2H, d, J = 3.4 Hz), 3.70 (1H, t, J = 2.6 Hz), 2.94 (2H, t, J = 7.8 Hz), 2.32 (2H, t, J = 7.3 Hz), 1.64–1.56 (4H, m), 1.36–1.25 (2H, m); MS (EI) *m/z*: 244 (M–-HCl); Anal. ($C_{15}H_{20}N_2O$·HCl·1/8H_2O) C, H, N.

The crude solid of **17** was recrystallized from $CHCl_3$–*n*-hexane to give 12 mg of **17** as colorless needles: mp 56–57 °C; ^{1}H NMR ($CDCl_3$, 400 MHz, δ; ppm) 7.51 (2H, d, J = 8.3 Hz), 7.32 (2H, t, J = 7.8 Hz), 7.11–7.10 (2H, m), 3.43 (4H, d, J = 2.4 Hz), 2.55 (2H, t, J = 7.3 Hz), 2.37 (2H, t, J = 7.4 Hz), 2.22 (2H, t, J = 2.3 Hz), 1.79–1.75 (2H, m), 1.54–1.52 (2H, m), 1.45–1.43 (2H, m); MS (EI) *m/z*: 281 (M^+); Anal. ($C_{18}H_{22}N_2O$) C, H, N.

7-Hydroxysulfamoylheptanoic Acid Phenylamide (6). Steps 1 and 2: Preparation of 7-Chlorosulfonylheptanoic Acid Ethyl Ester (60). To an aqueous solution (7 mL) of anhydrous sodium sulfite (2.03 g, 16.1 mmol) was added a solution of 7-bromoheptanoic acid ethyl ester (**59**, 2.0 g, 8.43 mmol) in EtOH (5 mL), and the solution was boiled under reflux with stirring for 2 h. The solution was evaporated to dryness, and the solid was dried in vacuo at 60 °C. This white solid was placed in a flask, toluene (30 mL) was added followed by a catalytic amount of DMF, and then thionyl chloride (6.2 mL, 85.0 mmol) was added dropwise. The mixture was boiled under reflux with stirring for 5 h, diluted with AcOEt, washed with aqueous saturated cold water and brine, and dried over $MgSO_4$. Filtration and concentration in vacuo and purification by silica gel flash chromatography (*n*-hexane/AcOEt = 4/1) gave 2.02 g (93%) of **60**: ^{1}H NMR ($CDCl_3$, 400 MHz, δ; ppm) 4.13 (2H, q, J = 7.1 Hz), 3.66 (2H, t, J = 7.8 Hz), 2.31 (2H, t, J = 7.3 Hz), 2.06 (2H, quintet, J = 7.8 Hz), 1.66 (2H, quintet, J = 7.3 Hz), 1.53 (2H, quintet, J = 7.8 Hz), 1.41 (2H, quintet, J = 7.1 Hz), 1.26 (2H, quintet, J = 7.1 Hz).

Steps 3, 4, and 5: Preparation of 7-(2-Tetrahydropyranyloxysulfamoyl)heptanoic Acid Phenylamide (61). To a mixture of *O*-(2-tetrahydropyranyl)hydroxylamine (251 mg, 2.14 mmol), a catalytic amount of 4-(dimethylamino)pyridine, pyridine (1 mL), and CH_2Cl_2 (10 mL) was added a solution of **60** (500 mg, 1.95 mmol) obtained above in CH_2Cl_2 (10 mL), and the mixture was stirred at room temperature for 5 h. The reaction mixture was poured into water and extracted with AcOEt. The AcOEt layer was separated, washed with water, saturated aqueous $NaHCO_3$ and brine, and dried over Na_2SO_4. Filtration and concentration in vacuo and purification by silica gel flash chromatography (*n*-hexane/AcOEt = 2/1) gave 618 mg (94%) of the sulfonamide as a crude oil.

To a solution of the sulfonamide(615 mg, 1.82 mmol) obtained above in EtOH (3 mL) was added 2 N aqueous NaOH (3.0 mL, 6.0 mmol). The mixture was stirred overnight at room temperature. The solvent was removed by evaporation in vacuo, and water was added to the residue. The mixture was neutralized with 2 N aqueous HCl (3.0 mL, 6.0 mmol) with cooling in an ice–water bath, and the mixture was extracted with AcOEt. The AcOEt layer was separated, washed with water and brine, and dried over Na_2SO_4. Filtration and concentration in vacuo gave 482 mg (86%) of the carboxylic acid as a white solid: ^{1}H NMR ($CDCl_3$, 400 MHz, δ; ppm) 7.40 (1H, broad s), 5.08 (1H, m), 3.93 (1H, m), 3.66 (1H, m), 3.21 (2H, m), 2.37 (2H, t, J = 7.3 Hz), 1.90–1.35 (14H, m).

Compound **61** was prepared from the carboxylic acid obtained above and aniline using the procedure described for **13** in 88% yield: ^{1}H NMR (DMSO-d_6, 400 MHz, δ; ppm) 10.04 (1H, broad s), 9.85 (1H, broad s), 7.58 (2H, d, J = 8 Hz), 7.28 (2H, t, J = 7.8 Hz), 7.01 (1H, t, J = 7.6 Hz), 4.88 (1H, m), 3.81 (1H, m), 3.52 (1H, m), 3.19–3.09 (2H, m), 2.30 (2H, t, J = 7.3 Hz), 1.80–1.25 (14H, m).

Step 6: Preparation of 7-Hydroxysulfamoylheptanoic Acid Phenylamide (6). Compound **6** was prepared from **61** obtained above using the procedure described for **12** (step 2) in 61% yield: mp 137–139 °C; ^{1}H NMR (DMSO-d_6, 400 MHz, δ; ppm) 9.85 (1H, broad s), 9.51 (1H, d, J = 3.2 Hz), 9.13 (1H, d, J = 3.2 Hz), 7.58 (2H, d, J = 8 Hz), 7.28 (2H, t, J = 7.8 Hz), 7.01 (1H, t, J = 7.3 Hz), 3.09 (2H, t, J = 7.6 Hz), 2.30 (2H, t, J = 7.3 Hz), 1.68 (2H, quintet, J = 8 Hz), 1.59 (2H, quintet, J = 7.6 Hz), 1.41 (2H, quintet, J = 7.8 Hz), 1.32 (2H, quintet, J = 7.1 Hz); Anal. ($C_{13}H_{20}N_2O_4S$·1/20H_2O) C, H, N.

Thioacetic acid S–(6-phenylcarbamoylhexyl) Ester (8a). Steps 1, 2, and 3: Preparation of 7-Bromoheptanoic Acid Phenylamide (64c). 7-Bromoheptanoic acid was prepared from **59** using the procedure described for **6** (step 4) in 99% yield. In this case, LiOH was used instead of NaOH: ^{1}H NMR ($CDCl_3$, 400 MHz, δ; ppm) 3.41 (2H, t, J = 6.8 Hz), 2.37 (2H, t, J = 7.3 Hz), 1.87 (2H, quintet, J = 6.8 Hz), 1.66 (2H, quintet, J = 7.6 Hz), 1.54–1.32 (4H, m).

To a suspension of 7-bromoheptanoic acid (2.64 g, 12.6 mmol) obtained above in CH_2Cl_2 (30 mL) were added oxalyl chloride (1.65 mL, 18.9 mmol) and a catalytic amount of DMF. The mixture was stirred at room temperature for 2 h. The solvent was removed by evaporation in vacuo to give acid chloride **62c**.

To a solution of aniline (3.50 g, 37.6 mmol) and triethylamine (5.30 mL, 38.1 mmol) in CH_2Cl_2 (40 mL) was added a solution of **62c** obtained above in CH_2Cl_2 (10 mL) dropwise cooling in an ice–water bath. The mixture was stirred at room temperature for 1 h. It was diluted with AcOEt and washed with aqueous saturated $NaHCO_3$, water, and brine, before being dried over $MgSO_4$. Filtration and concentration in vacuo and purification by silica gel flash chromatography (*n*-hexane/AcOEt = 3/1) gave 3.13 g (87%) of **64c**: ^{1}H NMR ($CDCl_3$, 400 MHz, δ; ppm) 7.51 (2H, d, J = 8.1 Hz), 7.32 (2H, t, J = 7.6 Hz), 7.15 (1H, broad s), 7.10 (1H, t, J = 7.6 Hz), 3.41 (2H, t, J = 6.8 Hz), 2.36 (2H, t, J = 7.3 Hz), 1.87 (2H, quintet, J = 7.1 Hz), 1.75 (2H, quintet, J = 7.3 Hz), 1.49 (2H, quintet, J = 7.6 Hz), 1.41 (2H, quintet, J = 6.8 Hz).

Step 4: Preparation of Thioacetic acid *S*-(6-Phenylcarbamoylhexyl) Ester (8a). Compound **8a** was prepared from **64c** obtained above using the procedure described for **15** in 98% yield: mp 80–81 °C; ^{1}H NMR ($CDCl_3$, 400 MHz, δ; ppm) 7.51 (2H, d, J = 8 Hz), 7.32 (2H, t, J = 7.3 Hz), 7.22

(1H, broad s), 7.10 (1H, t, J = 7.3 Hz), 2.86 (2H, t, J = 7.1 Hz), 2.35 (2H, t, J = 7.3 Hz), 2.32 (3H, s), 1.73 (2H, quintet, J = 7.1 Hz), 1.59 (2H, quintet, J = 7.1 Hz), 1.40 (4H, m); MS (EI) *m/z*: 279 (M^+); Anal. ($C_{15}H_{21}NO_2S$) C, H, N.

7-Mercaptoheptanoic Acid Phenylamide (7) and 7-(6-Phenylcarbamoylhexyldisulfanyl)heptanoic Acid Phenylamide (37). Compounds **7** and **37** were prepared from **8a** using the procedure described for **6** (step 4) in 87% and 4% yield, respectively.

7: mp 88–89 °C; ^{1}H NMR ($CDCl_3$, 400 MHz, δ; ppm) 7.51 (2H, d, J = 8 Hz), 7.32 (2H, t, J = 7.6 Hz), 7.12 (1H, broad s), 7.10 (1H, t, J = 7.1 Hz), 2.53 (2H, q, J = 7.3 Hz), 2.36 (2H, t, J = 7.6 Hz), 1.74 (2H, quintet, J = 7.1 Hz), 1.63 (2H, quintet, J = 7.1 Hz), 1.42 (4H, m), 1.33 (1H, t, J = 7.8 Hz); MS (EI) *m/z*: 237 (M^+); Anal. ($C_{13}H_{19}NOS$) C, H, N.

37: mp 105–107 °C; ^{1}H NMR ($CDCl_3$, 400 MHz, δ; ppm) 7.51 (4H, d, J = 8 Hz), 7.41 (2H, broad s), 7.30 (4H, t, J = 7.8 Hz), 7.09 (2H, t, J = 7.3 Hz), 2.68 (4H, t, J = 7.3 Hz), 2.36 (4H, t, J = 7.6 Hz), 1.74 (4H, quintet, J = 7.3 Hz), 1.69 (4H, quintet, J = 7.1 Hz), 1.50–1.34 (8H, m); MS (EI) *m/z*: 472 (M^+); Anal. ($C_{26}H_{36}N_2O_2S_2$) C, H, N.

Compounds**19–21**, **24**, **26–31**, and **32** were prepared from **62** and an appropriate aromatic amine using the procedure described for **8a** and **7**.

8-Mercaptooctanoic acid phenylamide (19): mp 84–86 °C; ^{1}H NMR ($CDCl_3$, 400 MHz, δ; ppm) 7.51 (2H, d, J = 8 Hz), 7.32 (2H, t, J = 7.6 Hz), 7.14 (1H, broad s), 7.10 (1H, t, J = 7.3 Hz), 2.52 (2H, q, J = 7.3 Hz), 2.35 (2H, t, J = 7.6 Hz), 1.73 (2H, quintet, J = 7.3 Hz), 1.61 (2H, quintet, J = 7.1 Hz), 1.46–1.34 (6H, m), 1.33 (1H, t, J = 7.8 Hz); MS (EI) *m/z*: 251 (M^+); Anal. ($C_{14}H_{21}NOS$) C, H, N.

6-Mercaptohexanoic acid phenylamide (20): mp 84–85 °C; ^{1}H NMR ($CDCl_3$, 400 MHz, δ; ppm) 7.51 (2H, d, J = 8.1 Hz), 7.32 (2H, t, J = 7.6 Hz), 7.16 (1H, broad s), 7.11 (1H, t, J = 7.8 Hz), 2.55 (2H, q, J = 7.1 Hz), 2.37 (2H, t, J = 7.3 Hz), 1.75 (2H, quintet, J = 7.8 Hz), 1.68 (2H, quintet, J = 7.6 Hz), 1.56–1.40 (2H, m), 1.35 (1H, t, J = 7.8 Hz); MS (EI) *m/z*: 223 (M^+); Anal. ($C_{12}H_{17}NOS$) C, H, N.

5-Mercaptopentanoic acid phenylamide (21): mp 120–121 °C; ^{1}H NMR ($CDCl_3$, 400 MHz, δ; ppm) 7.51 (2H, d, J = 7.6 Hz), 7.33 (2H, t, J = 8 Hz), 7.16 (1H, broad s), 7.11 (1H, t, J = 7.8 Hz), 2.58 (2H, q, J = 6.4 Hz), 2.39 (2H, t, J = 6.8 Hz), 1.85 (2H, quintet, J = 7.8 Hz), 1.71 (2H, quintet, J = 7.6 Hz), 1.39 (1H, t, J = 8 Hz); MS (EI) *m/z*: 209 (M^+); Anal. ($C_{11}H_{15}NOS \cdot 1/12H_2O$) C, H, N.

7-Mercaptoheptanoic acid (4-dimethylaminophenyl)amide (24): mp 121–122 °C; ^{1}H NMR ($CDCl_3$, 400 MHz, δ; ppm) 7.51 (2H, d, J = 9 Hz), 6.96 (1H, broad s), 6.70 (2H, d, J = 9 Hz), 2.91 (6H, s), 2.53 (2H, q, J = 7.3 Hz), 2.32 (2H, t, J = 7.3 Hz), 1.73 (2H, quintet, J = 7.4 Hz), 1.63 (2H, quintet, J = 7.6 Hz), 1.50–1.35 (4H, m), 1.33 (1H, t, J = 7.8 Hz); MS (EI) *m/z*: 280 (M^+); Anal. ($C_{15}H_{24}N_2OS$) C, H, N.

7-Mercaptoheptanoic acid 3-biphenylylamide (26): mp 91–92 °C; ^{1}H NMR ($CDCl_3$, 400 MHz, δ; ppm) 7.78 (1H, s), 7.59 (2H, d, J = 7.6 Hz), 7.49 (1H, d, J = 7.4 Hz), 7.47–7.30 (5H, m), 7.18 (1H, broad s), 2.53 (2H, q, J = 7.3 Hz), 2.39 (2H, t, J = 7.3 Hz), 1.76 (2H, quintet, J = 7.1 Hz), 1.64 (2H, quintet, J = 7.3 Hz), 1.50–1.37 (4H, m), 1.33 (1H, t, J = 7.6 Hz); MS (EI) *m/z*: 313 (M^+); Anal. ($C_{19}H_{23}NOS$) C, H, N.

7-Mercaptoheptanoic acid (4-phenoxyphenyl)amide (27): mp 87–89 °C; ^{1}H NMR ($CDCl_3$, 400 MHz, δ; ppm) 7.47 (2H, d, J = 8.8 Hz), 7.32 (2H, t, J = 7.8 Hz), 7.12 (1H, broad s), 7.08 (1H, t, J = 7.3 Hz), 6.98 (4H, d, J = 8.8 Hz), 2.53 (2H, q, J = 7.3 Hz), 2.36 (2H, t, J = 7.6 Hz), 1.75 (2H, quintet, J = 7.1 Hz), 1.64 (2H, quintet, J = 7.1 Hz), 1.50–1.37 (4H, m), 1.33 (1H, t, J = 7.8 Hz); MS (EI) *m/z*: 329 (M^+); Anal. ($C_{19}H_{23}NO_2S$) C, H, N.

7-Mercaptoheptanoic acid (3-phenoxyphenyl)amide (28): mp 68–69 °C; ^{1}H NMR ($CDCl_3$, 400 MHz, δ; ppm) 7.34 (2H, t, J = 7.6 Hz), 7.30–7.18 (3H, m), 7.16 (1H, broad s), 7.11 (1H, t, J = 7.2 Hz), 7.02 (2H, d, J = 8.5 Hz), 6.74 (1H, s), 2.52 (2H, q, J = 7.3 Hz), 2.33 (2H, t, J = 7.3 Hz), 1.71 (2H, quintet, J = 7.3 Hz), 1.62 (2H, quintet, J = 7.1 Hz), 1.50–1.34 (4H, m), 1.32 (1H, t, J = 7.6 Hz); MS (EI) *m/z*: 329 (M^+); Anal. ($C_{19}H_{23}NO_2S$) C, H, N.

7-Mercaptoheptanoic acid 3-pyridinylamide (29): mp 74–76 °C; ^{1}H NMR ($CDCl_3$, 400 MHz, δ; ppm) 8.54 (1H, d, J = 2.4 Hz), 8.35 (1H, d, J = 4.4 Hz), 8.19 (1H, d, J = 8.3 Hz), 7.31 (1H, broad s), 7.28 (1H, dd, J = 4.4, 8.3 Hz), 2.53 (2H, q, J = 7.1 Hz), 2.40 (2H, t, J = 7.3 Hz), 1.75 (2H, quintet, J = 7.6 Hz), 1.64 (2H, quintet, J = 7.1 Hz), 1.50–1.36 (4H, m), 1.33 (1H, t, J = 7.6 Hz); MS (EI) *m/z*: 237 (M^+); Anal. ($C_{12}H_{18}N_2OS$) C, H, N.

7-Mercaptoheptanoic acid 3-quinolinylamide (30): mp 75–76 °C; ^{1}H NMR ($CDCl_3$, 400 MHz, δ; ppm) 8.79 (1H, d, J = 2.7 Hz), 8.72 (1H, d, J = 2.7 Hz), 8.04 (1H, d, J = 8.3 Hz), 7.80 (1H, d, J = 8.3 Hz), 7.64 (1H, t, J = 7.1 Hz), 7.54 (1H, t, J = 7.1 Hz), 7.50 (1H, broad s), 2.54 (2H, q, J = 7.1 Hz), 2.47 (2H, t, J = 7.3 Hz), 1.80 (2H, quintet, J = 7.3 Hz), 1.64 (2H, quintet, J = 7.3 Hz), 1.53–1.37 (4H, m), 1.34 (1H, t, J = 7.8 Hz); MS (EI) *m/z*: 288 (M^+); Anal. ($C_{16}H_{20}N_2OS$) C, H, N.

7-Mercaptoheptanoic acid (4-phenyl-2-thiazolyl)amide (31): mp 149–150 °C; ^{1}H NMR ($CDCl_3$, 400 MHz, δ; ppm) 10.36 (1H, broad s), 7.83 (2H, d, J = 7.1 Hz), 7.43 (2H, t, J = 7.3 Hz), 7.16 (1H, s), 2.49 (2H, q, J = 7.1 Hz), 2.14 (2H, t, J = 7.6 Hz), 1.65–1.50 (4H, m), 1.32 (1H, t, J = 7.6 Hz), 1.30 (2H, quintet, J = 7.3 Hz), 1.15 (2H, quintet, J = 7.1 Hz); MS (EI) *m/z*: 320 (M^+); Anal. ($C_{16}H_{20}N_2OS_2 \cdot 1/10H_2O$) C, H, N.

7-Mercaptoheptanoic acid 2-benzothiazolylamide (32): mp 141–142 °C; ^{1}H NMR ($CDCl_3$, 400 MHz, δ; ppm) 10.71 (1H, broad s), 7.86 (1H, d, J = 7.9 Hz), 7.77 (1H, d, J = 8 Hz), 7.46 (1H, t, J = 8.3 Hz), 7.34 (1H, t, J = 8.3 Hz), 2.49 (2H, t, J = 7.1 Hz), 2.48 (2H, q, J = 7.3 Hz), 1.72 (2H, quint, J = 7.6 Hz), 1.57 (2H, quint, J = 7.3 Hz), 1.40–1.25 (5H, m); MS (EI) *m/z*: 294 (M^+); Anal. ($C_{14}H_{18}N_2OS_2$) C, H, N.

7-Mercaptoheptanoic Acid 4-Biphenylylamide (25). Step 1: Preparation of 7-Bromoheptanoic Acid (4-Bromophenyl)amide (64a). Compound **64a** was prepared from **62c** and 4-bromoaniline using the procedure described for **8a** (step 3) in 86% yield: ^{1}H NMR ($CDCl_3$, 400 MHz, δ; ppm) 7.42 (4H, s), 7.14 (1H, broad s), 3.41 (2H, t, J = 6.6 Hz), 2.36 (2H, t, J = 7.6 Hz), 1.87 (2H, quintet, J = 7.1 Hz), 1.74 (2H, quintet, J = 7.3 Hz), 1.49 (2H, quintet, J = 7.3 Hz), 1.40 (2H, quintet, J = 6.8 Hz).

Step 2: Preparation of 7-Bromoheptanoic Acid 4-Biphenylylamide (64b). To a suspension of **64a** (500 mg, 1.38 mmol) obtained above in 1-methyl-2-pyrrolidinone (8 mL) and water (4 mL) were added phenylboronic acid (252 mg, 2.07 mmol), tetrakis(triphenylphosphine)palladium(0) (160 mg, 0.14 mmol), and $NaHCO_3$ (235 mg, 2.80 mmol). The mixture was heated at 80 °C for 1 h. The solution was diluted with AcOEt, washed with saturated aqueous $NaHCO_3$, water, and brine, and dried over Na_2SO_4. Filtration and concentration in vacuo and purification by silica gel flash chromatography (*n*-hexane/AcOEt = 3/1) gave 91 mg (18%) of **64b** as a white solid: ^{1}H NMR ($CDCl_3$, 400 MHz, δ; ppm) 7.65–7.50 (6H, m), 7.43 (2H, t, J = 7.6 Hz), 7.33 (1H, t, J = 7.1 Hz), 7.20 (1H, broad s), 3.42 (2H, t, J = 6.6 Hz), 2.39 (2H, t, J = 7.3 Hz), 1.88 (2H, quintet, J = 7.1 Hz), 1.77 (2H, quintet, J = 7.3 Hz), 1.50 (2H, quintet, J = 7.1 Hz), 1.43 (2H, quintet, J = 6.4 Hz).

Steps 3 and 4: Preparation of 7-Mercaptoheptanoic Acid 4-Biphenylylamide (25). Compound **25** was prepared from **64b** obtained above using the procedure described for **15** and **6** (step 4) in 48% yield: mp 114–115 °C; ^{1}H NMR ($CDCl_3$, 400 MHz, δ; ppm) 7.64–7.52 (6H, m), 7.43 (2H, t, J = 7.6 Hz), 7.33 (1H, t, J = 7.3 Hz), 7.17 (1H, broad s), 2.54 (2H, q, J = 7.4 Hz), 2.39 (2H, t, J = 7.3 Hz), 1.76 (2H, quintet, J = 7.3 Hz), 1.64 (2H, quintet, J = 7.3 Hz), 1.52–1.37 (4H, m), 1.34 (1H, t, J = 7.6 Hz); MS (EI) *m/z*: 313 (M^+); Anal. ($C_{19}H_{23}NOS \cdot 1/5H_2O$) C, H, N.

7-Methylsulfanylheptanoic Acid Phenylamide (9). To a solution of **64c** (300 mg, 1.06 mmol) in EtOH (10 mL) was added methylmercaptan sodium salt (15% in water, 1.50 g, 3.21 mmol), and the solution was stirred at room temperature for 5 h. The reaction mixture was diluted with AcOEt, washed with water and brine, and dried over $MgSO_4$. Filtration and concentration in vacuo and purification by silica gel flash

chromatography (*n*-hexane/AcOEt = 2/1) gave 262 mg (99%) of **9** as a crude solid. The solid was recrystallized from *n*-hexane–AcOEt and collected by filtration to give 217 mg of **9** as a colorless crystal: mp 50–51 °C; ^{1}H NMR ($CDCl_3$, 400 MHz, δ; ppm) 7.51 (2H, d, J = 8 Hz), 7.32 (2H, t, J = 7.8 Hz), 7.16 (1H, broad s), 7.10 (1H, t, J = 7.6 Hz), 2.49 (2H, t, J = 7.1 Hz), 2.36 (2H, t, J = 7.3 Hz), 2.09 (3H, s), 1.74 (2H, quintet, J = 7.3 Hz), 1.61 (2H, quintet, J = 7.3 Hz), 1.42 (4H, m); MS (EI) *m/z*: 251 (M^+); Anal. ($C_{14}H_{21}NOS$) C, H, N.

7-Methanesulfonylheptanoic Acid Phenylamide (11). To a solution of **9** (80 mg, 0.32 mmol) in CH_2Cl_2 (3 mL) was added 3-chloroperoxybenzoic acid (65%, 180 mg, 0.68 mmol). The mixture was stirred overnight at room temperature. Next, saturated aqueous $NaHCO_3$ and saturated aqueous $Na_2S_2O_3$ were added, and the mixture was stirred at room temperature for 1 h. It was then poured into water and extracted with $CHCl_3$. The $CHCl_3$ layer was separated, washed with water and brine, and dried over Na_2SO_4. Filtration and concentration in vacuo and separation by silica gel flash chromatography (*n*-hexane/AcOEt = 1/3) gave 63 mg (70%) of **11** as a crude solid. The solid was recrystallized from *n*-hexane-AcOEt and collected by filtration to give 50 mg of **11** as a colorless crystal: mp 121–123 °C; ^{1}H NMR ($CDCl_3$, 400 MHz, δ; ppm) 7.51 (2H, d, J = 7.8 Hz), 7.32 (2H, t, J = 7.6 Hz), 7.17 (1H, brs), 7.11 (1H, t, J = 7.3 Hz), 3.01 (2H, t, J = 7.8 Hz), 2.89 (3H, s), 2.37 (2H, t, J = 7.3 Hz), 1.88 (2H, quint, J = 7.6 Hz), 1.76 (2H, quint, J = 7.6 Hz), 1.60–1.35 (4H, m); MS (EI) *m/z*: 283 (M^+); Anal. ($C_{14}H_{21}NO_3S$) C, H, N.

6-Phenoxy-1-hexanethiol (22). Step 1: Preparation of 6-Phenoxy-1-hexanol (67). To a solution of phenol (2.10 g, 22.31 mmol) and 6-bromo-1-hexanol (**65**, 2.00 g, 11.05 mmol) in DMF (30 mL) was added K_2CO_3 (3.10 g, 22.4 mmol), and the mixture was stirred at 80 °C for 1 h. The reaction mixture was diluted with AcOEt and washed with water and brine, before being dried over Na_2SO_4. Filtration and concentration in vacuo and purification by silica gel flash chromatography (*n*-hexane/AcOEt = 2/1) gave 2.06 g (96%) of **67** as a white solid: ^{1}H NMR ($CDCl_3$, 400 MHz, δ; ppm) 7.28 (2H, t, J = 7.8 Hz), 6.93 (1H, t, J = 7.3 Hz), 6.89 (2H, d, J = 8.6 Hz), 3.96 (2H, t, J = 6.6 Hz), 3.67 (2H, m), 1.80 (2H, quintet, J = 6.8 Hz), 1.61 (2H, quintet, J = 7.3 Hz), 1.56–1.36 (4H, m), 1.27 (1H, m).

Step 2: Preparation of (6-Bromohexyloxy)benzene. To a solution of **67** (1.75 g, 9.01 mmol) obtained above and carbon tetrabromide (3.00 g, 9.05 mmol) in CH_2Cl_2 (50 mL) was added triphenylphosphine (2.60 g, 9.91 mmol) with cooling in an ice–water bath. The solution was stirred at room temperature for 1 h and concentrated in vacuo. To the residue was added *n*-hexane (30 mL), and the slurry was filtered. After the solid was washed with *n*-hexane (10 mL), the combined filtrates were concentrated in vacuo. The residue was purified by silica gel flash chromatography (*n*-hexane/AcOEt = 1/30) to give 1.45 g (63%) of (6-bromohexyloxy)benzene as a colorless oil: ^{1}H NMR ($CDCl_3$, 400 MHz, δ; ppm) 7.28 (2H, t, J = 7.6 Hz), 6.93 (1H, t, J = 7.3 Hz), 6.89 (2H, d, J = 8.5 Hz), 3.96 (2H, t, J = 6.3 Hz), 3.43 (2H, t, J = 6.8 Hz), 1.90 (2H, quintet, J = 6.8 Hz), 1.80 (2H, quintet, J = 6.4 Hz), 1.56–1.46 (4H, m).

Steps 3 and 4: Preparation of 6-Phenoxy-1-hexanethiol (22). Compound **22** was prepared from (6-bromohexyloxy)-benzene obtained above using the procedure described for **15** and **6** (step 4) in 45% yield: colorless oil; ^{1}H NMR ($CDCl_3$, 400 MHz, δ; ppm) 7.28 (2H, t, J = 7.3 Hz), 6.93 (1H, t, J = 7.6 Hz), 6.89 (2H, d, J = 7.8 Hz), 3.96 (2H, t, J = 6.4 Hz), 2.54 (2H, q, J = 7.1 Hz), 1.79 (2H, quintet, J = 6.6 Hz), 1.65 (2H, quintet, J = 6.8 Hz), 1.54–1.44 (4H, m), 1.34 (1H, t, J = 7.8 Hz); MS (EI) *m/z*: 210 (M^+); HRMS calcd for $C_{12}H_{18}OS$ 210.108, found 210.108.

Compounds**23**, **33–35**, and **36** were prepared from an appropriate aromatic carboxylic acid and 6-amino-1-hexanol (**66**) using the procedure described for **13**, **22** (step 2), **15**, and **6** (step 4).

***N*-(6-Mercaptohexyl)benzamide (23)**: mp 43–44 °C; ^{1}H NMR ($CDCl_3$, 400 MHz, δ; ppm) 7.77 (2H, d, J = 7.2 Hz), 7.50 (1H, t, J = 7.2 Hz), 7.43 (2H, t, J = 6.8 Hz), 6.20 (1H, broad s), 3.47 (2H, q, J = 6.4 Hz), 2.54 (2H, q, J = 7.6 Hz), 1.68–1.58 (4H, m), 1.50–1.36 (4H, m), 1.52–1.37 (4H, m), 1.34 (1H, t, J = 7.8 Hz); MS (EI) *m/z*: 237 (M^+); Anal. ($C_{13}H_{19}NOS\cdot 1/6H_2O$) C, H, N.

4-Dimethylamino-*N*-(6-mercaptohexyl)benzamide (33): mp 103–104 °C; ^{1}H NMR ($CDCl_3$, 400 MHz, δ; ppm) 7.66 (2H, t, J = 8.8 Hz), 6.67 (2H, d, J = 8.8 Hz), 5.95 (1H, s), 3.43 (2H, q, J = 6.4 Hz), 3.02 (1H, s), 2.53 (2H, q, J = 7.2 Hz), 1.67–1.54 (4H, m), 1.49–1.36 (4H, m), 1.32 (1H, t, J = 8 Hz); MS (EI) *m/z*: 280 (M^+); Anal. ($C_{15}H_{24}N_2OS$) C, H, N.

Naphthalene-2-carboxylic acid (6-mercaptohexyl)amide (34): mp 76–78 °C; ^{1}H NMR ($CDCl_3$, 400 MHz, δ; ppm) 8.28 (1H, s), 7.94–7.85 (3H, m), 7.82 (1H, d, J = 6.8 Hz), 7.58–7.53 (2H, m), 6.27 (1H, s), 3.52 (2H, q, J = 6.8 Hz), 2.54 (2H, q, J = 7.6 Hz), 1.70–1.62 (4H, m), 1.52–1.36 (4H, m), 1.34 (1H, t, J = 7.8 Hz); MS (EI) *m/z*: 287 (M^+); Anal. ($C_{17}H_{21}NOS$) C, H, N.

Benzofuran-2-carboxylic acid (6-mercaptohexyl)amide (35): mp 72–73 °C; ^{1}H NMR ($CDCl_3$, 400 MHz, δ; ppm) 7.68 (1H, d, J = 8 Hz), 7.50 (1H, d, J = 8.4 Hz), 7.46 (1H, s), 7.41 (1H, t, J = 8.4 Hz), 7.30 (1H, t, J = 8 Hz), 6.64 (1H, s), 3.49 (2H, q, J = 7.2 Hz), 2.54 (2H, q, J = 7.2 Hz), 1.72–1.58 (4H, m), 1.52–1.38 (4H, m), 1.34 (1H, t, J = 7.8 Hz); MS (EI) *m/z*: 277 (M^+); Anal. ($C_{15}H_{19}NO_2S$) C, H, N.

Indole-2-carboxylic acid (6-mercaptohexyl)amide (36): mp 128–130 °C; ^{1}H NMR ($CDCl_3$, 400 MHz, δ; ppm) 9.12 (1H, broad s), 7.65 (1H, d, J = 8 Hz), 7.44 (1H, d, J = 8.4 Hz), 7.29 (1H, t, J = 8 Hz), 7.14 (1H, t, J = 6.6 Hz), 6.82 (1H, s), 6.13 (1H, broad s), 3.49 (2H, q, J = 6.8 Hz), 2.54 (2H, q, J = 7.6 Hz), 1.70–1.60 (4H, m), 1.45–1.40 (4H, m), 1.34 (1H, t, J = 7.8 Hz); MS (EI) *m/z*: 276 (M^+); Anal. ($C_{15}H_{20}N_2OS$) C, H, N.

Thiopropionic Acid *S*-(6-Phenylcarbamoylhexyl) Ester (38). To a solution of **7** (200 mg, 0.84 mmol) and a catalytic amount of 4-(dimethylamino)pyridine in CH_2Cl_2 (2 mL) and pyridine (0.5 mL) was added propionyl chloride (220 μL, 2.53 mmol). The mixture was stirred at room temperature for 30 min and then diluted with AcOEt. The solution was washed with water and brine and dried over Na_2SO_4. Filtration and concentration in vacuo and separation by silica gel flash chromatography (*n*-hexane/AcOEt = 3/1) gave 238 mg (96%) of **38** as a crude solid. The solid was recrystallized from *n*-hexane-AcOEt and collected by filtration to give 184 mg of **38** as a colorless crystal: mp 54–55 °C; ^{1}H NMR ($CDCl_3$, 500 MHz, δ; ppm) 7.52 (2H, d, J = 7.9 Hz), 7.32 (2H, t, J = 7.9 Hz), 7.21 (1H, broad s), 7.10 (1H, t, J = 7.3 Hz), 2.86 (2H, t, J = 7.4 Hz), 2.57 (2H, q, J = 7.7 Hz), 2.35 (2H, t, J = 7.6 Hz), 1.74 (2H, quintet, J = 7.3 Hz), 1.59 (2H, quintet, J = 7.3 Hz), 1.46–1.33 (4H, m), 1.18 (3H, t, J = 7.7 Hz); MS (EI) *m/z*: 293 (M^+); Anal. ($C_{16}H_{23}NO_2S$) C, H, N.

Compounds **39–45**, **47–54**, and **55** were prepared from the corresponding thiols and an appropriate acid chloride using the procedure described for **38**.

Thiobutyric acid *S*-(6-phenylcarbamoylhexyl) ester (39): mp 45–46 °C; ^{1}H NMR ($CDCl_3$, 500 MHz, δ; ppm) 7.52 (2H, d, J = 8 Hz), 7.32 (2H, t, J = 7.6 Hz), 7.21 (1H, broad s), 7.10 (1H, t, J = 7.3 Hz), 2.86 (2H, t, J = 7 Hz), 2.52 (2H, t, J = 7.3 Hz), 2.35 (2H, t, J = 7.4 Hz), 1.73 (2H, quintet, J = 7.4 Hz), 1.69 (2H, sextet, J = 7.7 Hz), 1.59 (2H, quintet, J = 7.4 Hz), 1.48–1.33 (4H, m), 0.95 (3H, t, J = 7.3 Hz); MS (EI) *m/z*: 307 (M^+); Anal. ($C_{17}H_{25}NO_2S$) C, H, N.

Thioisobutyric acid *S*-(6-phenylcarbamoylhexyl) ester (40): mp 44–45 °C; ^{1}H NMR ($CDCl_3$, 400 MHz, δ; ppm) 7.52 (2H, d, J = 8 Hz), 7.32 (2H, t, J = 7.8 Hz), 7.22 (1H, broad s), 7.10 (1H, t, J = 7.3 Hz), 2.85 (2H, t, J = 7.3 Hz), 2.73 (1H, septet, J = 7 Hz), 2.35 (2H, t, J = 7.3 Hz), 1.73 (2H, quintet, J = 7.3 Hz), 1.59 (2H, quintet, J = 7.3 Hz), 1.46–1.36 (4H, m), 1.19 (6H, d, J = 7.6 Hz); MS (EI) *m/z*: 307 (M^+); Anal. ($C_{17}H_{25}NO_2S$) C, H, N.

2,2-Dimethylthiopropionic acid *S*-(6-phenylcarbamoylhexyl) ester (41): mp 57–59 °C; ^{1}H NMR ($CDCl_3$, 400 MHz, δ; ppm) 7.52 (2H, d, J = 8.1 Hz), 7.32 (2H, t, J = 7.6 Hz), 7.20 (1H, broad s), 7.10 (1H, t, J = 7.6 Hz), 2.82 (2H, t, J = 7.3 Hz), 2.35 (2H, t, J = 7.3 Hz), 1.73 (2H, quintet, J = 7.3

Hz), 1.58 (2H, quintet, J = 7.3 Hz), 1.46−1.36 (4H, m), 1.23 (9H, s); MS (EI) *m/z*: 321 (M^+); Anal. ($C_{18}H_{27}NO_2S$) C, H, N.

Cyclopropanecarbothioic acid *S*-(6-phenylcarbamoylhexyl) ester (42): mp 64−65 °C; ^{1}H NMR ($CDCl_3$, 500 MHz, δ; ppm) 7.52 (2H, d, J = 8.3 Hz), 7.32 (2H, t, J = 7.6 Hz), 7.22 (1H, broad s), 7.10 (1H, t, J = 7.3 Hz), 2.89 (2H, t, J = 7.3 Hz), 2.35 (2H, t, J = 7.3 Hz), 2.01 (1H, m), 1.73 (2H, quintet, J = 7 Hz), 1.59 (2H, quintet, J = 7.3 Hz), 1.45−1.35 (4H, m), 1.15 (2H, m), 0.94 (2H, m); MS (EI) *m/z*: 305 (M^+); Anal. ($C_{17}H_{23}NO_2S$) C, H, N.

Cyclopentanecarbothioic acid *S*-(6-phenylcarbamoylhexyl) ester (43): mp 59−60 °C; ^{1}H NMR ($CDCl_3$, 500 MHz, δ; ppm) 7.52 (2H, d, J = 7.9 Hz), 7.32 (2H, t, J = 7.9 Hz), 7.21 (1H, broad s), 7.10 (1H, t, J = 7.3 Hz), 2.97 (1H, quintet, J = 8 Hz), 2.85 (2H, t, J = 7.4 Hz), 2.35 (2H, t, J = 7.7 Hz), 1.93−1.67 (8H, m), 1.63−1.52 (4H, m), 1.47−1.33 (4H, m); MS (EI) *m/z*: 333 (M^+); Anal. ($C_{19}H_{27}NO_2S$) C, H, N.

Thiobenzoic acid *S*-(6-phenylcarbamoylhexyl) ester (44): mp 107−109 °C; ^{1}H NMR ($CDCl_3$, 400 MHz, δ; ppm) 7.97 (2H, d, J = 7.3 Hz), 7.57 (1H, t, J = 7.3 Hz), 7.52 (2H, d, J = 7.8 Hz), 7.45 (2H, t, J = 7.8 Hz), 7.31 (2H, t, J = 7.6 Hz), 7.21 (1H, broad s), 7.10 (1H, t, J = 7.3 Hz), 3.07 (2H, t, J = 7.3 Hz), 2.36 (2H, t, J = 7.3 Hz), 1.75 (2H, quintet, J = 7.3 Hz), 1.70 (2H, quintet, J = 7.3 Hz), 1.54−1.36 (4H, m); MS (EI) *m/z*: 341 (M^+); Anal. ($C_{20}H_{23}NO_2S$) C, H, N.

4-Nitrothiobenzoic acid *S*-(6-phenylcarbamoylhexyl) ester (45): mp 117−118 °C; ^{1}H NMR ($CDCl_3$, 400 MHz, δ; ppm) 8.30 (2H, d, J = 8.8 Hz), 8.11 (2H, d, J = 8.6 Hz), 7.51 (2H, d, J = 8.1 Hz), 7.32 (2H, t, J = 7.8 Hz), 7.16 (1H, broad s), 7.10 (1H, t, J = 7.3 Hz), 3.12 (2H, t, J = 7.3 Hz), 2.37 (2H, t, J = 7.3 Hz), 1.76 (2H, quintet, J = 7.6 Hz), 1.72 (2H, quintet, J = 7.3 Hz), 1.54−1.38 (4H, m); MS (EI) *m/z*: 386 (M^+); Anal. ($C_{20}H_{22}N_2O_4S$) C, H, N.

Thioisobutyric acid *S*-[6-(3-biphenylylcarbamoyl)hexyl] ester (47): mp 73−74 °C; ^{1}H NMR ($CDCl_3$, 500 MHz, δ; ppm) 7.79 (1H, s), 7.59 (2H, d, J = 7.4 Hz), 7.50 (1H, d, J = 8.3 Hz), 7.43 (2H, t, J = 7.3 Hz), 7.39 (1H, t, J = 8 Hz), 7.35 (1H, t, J = 7.3 Hz), 7.34 (1H, d, J = 7.3 Hz), 7.28 (1H, broad s), 2.85 (2H, t, J = 7.3 Hz), 2.73 (1H, septet, J = 6.8 Hz), 2.38 (2H, t, J = 7.3 Hz), 1.75 (2H, quintet, J = 7.6 Hz), 1.58 (2H, quintet, J = 7.3 Hz), 1.49−1.35 (4H, m), 1.18 (6H, d, J = 7.1 Hz); MS (EI) *m/z*: 390 (M^+); Anal. ($C_{23}H_{29}NO_2S$) C, H, N.

Thioisobutyric acid *S*-[6-(3-phenoxyphenylcarbamoyl)hexyl] ester (48): colorless oil; ^{1}H NMR ($CDCl_3$, 500 MHz, δ; ppm) 7.34 (2H, t, J = 7.6 Hz), 7.30−7.15 (4H, m), 7.11 (1H, t, J = 7.4 Hz), 7.02 (2H, d, J = 7.6 Hz), 6.74 (1H, d, J = 7.3 Hz), 2.84 (2H, t, J = 7.3 Hz), 2.73 (1H, septet, J = 7 Hz), 2.32 (2H, t, J = 7.3 Hz), 1.71 (2H, quintet, J = 7.4 Hz), 1.57 (2H, quintet, J = 7.4 Hz), 1.45−1.33 (4H, m), 1.18 (6H, d, J = 7 Hz); MS (EI) *m/z*: 399 (M^+); HRMS calcd for $C_{23}H_{29}NO_3S$ 399.187, found 399.191.

Thioisobutyric acid *S*-[6-(3-pyridinylcarbamoyl)hexyl] ester (49): mp 47−48 °C; ^{1}H NMR ($CDCl_3$, 500 MHz, δ; ppm) 8.55 (1H, d, J = 2.8 Hz), 8.34 (1H, d, J = 4.6 Hz), 8.21 (1H, d, J = 8.5 Hz), 7.56 (1H, broad s), 7.28 (1H, dd, J = 4.6, 8.3 Hz), 2.85 (2H, t, J = 7 Hz), 2.74 (1H, septet, J = 7 Hz), 2.39 (2H, t, J = 7.6 Hz), 1.75 (2H, quintet, J = 7.4 Hz), 1.59 (2H, quintet, J = 7.1 Hz), 1.45−1.35 (4H, m), 1.19 (6H, d, J = 6.8 Hz); MS (EI) *m/z*: 308 (M^+); Anal. ($C_{16}H_{24}N_2O_2S$) C, H, N.

Thioisobutyric acid *S*-[6-(3-quinolinylcarbamoyl)hexyl] ester (50): mp 67−68 °C; ^{1}H NMR ($CDCl_3$, 500 MHz, δ; ppm) 8.81 (1H, s), 8.73 (1H, d, J = 2.8 Hz), 8.03 (1H, d, J = 8.6 Hz), 7.80 (1H, d, J = 8.2 Hz), 7.70 (1H, broad s), 7.63 (1H, t, J = 7.1 Hz), 7.54 (1H, t, J = 7.3 Hz), 2.86 (2H, t, J = 7.3 Hz), 2.74 (1H, septet, J = 7 Hz), 2.46 (2H, t, J = 7.6 Hz), 1.79 (2H, quintet, J = 7.3 Hz), 1.60 (2H, quintet, J = 7.3 Hz), 1.50−1.35 (4H, m), 1.19 (6H, d, J = 6.7 Hz); MS (EI) *m/z*: 358 (M^+); Anal. ($C_{20}H_{26}N_2O_2S$) C, H, N.

Thioisobutyric acid *S*-[6-(4-phenyl-2-thiazolylcarbamoyl)hexyl] ester (51): mp 127−128 °C; ^{1}H NMR ($CDCl_3$, 500 MHz, δ; ppm) 10.48 (1H, broad s), 7.83 (2H, d, J = 7.3 Hz), 7.43 (2H, t, J = 7.3 Hz), 7.34 (1H, t, J = 7.4 Hz), 7.16 (1H, s), 2.81 (2H, t, J = 7.3 Hz), 2.74 (1H, septet, J = 7 Hz), 2.11 (2H, t, J = 7.6 Hz), 1.56 (2H, quintet, J = 7.6 Hz), 1.50 (2H, quintet, J = 7.3 Hz), 1.25 (2H, quintet, J = 7.6 Hz), 1.19 (6H, d, J = 7 Hz), 1.13 (2H, quintet, J = 7.3 Hz); MS (EI) *m/z*: 383 (M^+); Anal. ($C_{20}H_{26}N_2O_2S_2$) C, H, N.

Thioisobutyric acid *S*-[6-(2-benzothiazolylcarbamoyl)hexyl] ester (52): mp 106−107 °C; ^{1}H NMR ($CDCl_3$, 500 MHz, δ; ppm) 10.41 (1H, broad s), 7.85 (1H, d, J = 7.4 Hz), 7.77 (1H, d, J = 7.9 Hz), 7.46 (1H, dt, J = 1.2, 7.1 Hz), 7.34 (1H, dt, J = 1, 7.3 Hz), 2.81 (2H, t, J = 7.4 Hz), 2.73 (1H, septet, J = 7.1 Hz), 2.47 (2H, t, J = 7.7 Hz), 1.72 (2H, quintet, J = 7.3 Hz), 1.53 (2H, quintet, J = 7.1 Hz), 1.38−1.27 (4H, m), 1.18 (6H, d, J = 7 Hz); MS (EI) *m/z*: 364 (M^+); Anal. ($C_{18}H_{24}N_2O_2S_2$) C, H, N.

Thioisobutyric acid *S*-{6-[(2-naphthalenecarbonyl)amino]hexyl} ester (53): mp 70−71 °C; ^{1}H NMR ($CDCl_3$, 500 MHz, δ; ppm) 8.29 (1H, s), 7.93 (1H, d, J = 7.1 Hz), 7.90 (1H, d, J = 7.3 Hz), 7.88 (1H, d, J = 7.3 Hz), 7.84 (1H, d, J = 7 Hz), 7.57 (1H, t, J = 6.7 Hz), 7.54 (1H, t, J = 6.7 Hz), 6.36 (1H, broad s), 3.51 (2H, q, J = 6.4 Hz), 2.87 (2H, t, J = 7.3 Hz), 2.73 (1H, septet, J = 6.7 Hz), 1.67 (2H, quintet, J = 7.1 Hz), 1.60 (2H, quintet, J = 6.7 Hz), 1.50−1.38 (4H, m), 1.18 (6H, d, J = 6.8 Hz); MS (EI) *m/z*: 357 (M^+); Anal. ($C_{21}H_{27}NO_2S$) C, H, N.

Thioisobutyric acid *S*-{6-[(2-benzofurancarbonyl)amino]hexyl} ester (54): mp 67−68 °C; ^{1}H NMR ($CDCl_3$, 500 MHz, δ; ppm) 7.67 (1H, d, J = 7.7 Hz), 7.50 (1H, d, J = 7.6 Hz), 7.46 (1H, d, J = 1 Hz), 7.41 (1H, dt, J = 1.2, 7.3 Hz), 7.29 (1H, t, J = 7.6 Hz), 6.66 (1H, broad s), 3.48 (2H, q, J = 7 Hz), 2.86 (2H, t, J = 7.4 Hz), 2.73 (1H, septet, J = 7.1 Hz), 1.66 (2H, quintet, J = 7 Hz), 1.59 (2H, quintet, J = 7 Hz), 1.48−1.37 (4H, m), 1.18 (6H, d, J = 6.7 Hz); MS (EI) *m/z*: 347 (M^+); Anal. ($C_{19}H_{25}NO_3S$) C, H, N.

Thioisobutyric acid *S*-{6-[(1*H*-2-indolecarbonyl)amino]hexyl} ester (55): mp 142−143 °C; ^{1}H NMR ($CDCl_3$, 500 MHz, δ; ppm) 9.37 (1H, broad s), 7.65 (1H, d, J = 7.3 Hz), 7.44 (1H, d, J = 7.6 Hz), 7.29 (1H, t, J = 7 Hz), 7.14 (1H, t, J = 7.9 Hz), 6.86 (1H, s), 6.30 (1H, broad s), 3.49 (2H, q, J = 6.1 Hz), 2.87 (2H, t, J = 7.1 Hz), 2.74 (1H, septet, J = 7 Hz), 1.65 (2H, quintet, J = 7 Hz), 1.60 (2H, quintet, J = 7 Hz), 1.50−1.36 (4H, m), 1.19 (6H, d, J = 7 Hz); MS (EI) *m/z*: 346 (M^+); Anal. ($C_{19}H_{26}N_2O_2S$) C, H, N.

2,2-Dimethylpropionic Acid 6-Phenylcarbamoylhexylsulfanylmethyl Ester (46). To a suspension of sodium hydride (60%, 40.0 mg, 1.00 mmol) in DMF (2 mL) was added a solution of **7** (200 mg, 0.84 mmol) in DMF (3 mL) dropwise with cooling in an ice−water bath. The mixture was stirred for 30 min at 0 °C, and a solution of chloromethyl pivalate (134 μL, 0.93 mmol) in DMF (2 mL) was added at 0 °C. The solution was stirred at room temperature for 1 h. The reaction mixture was poured into ice−water and extracted with AcOEt. The AcOEt layer was separated, washed with water and brine, and dried over Na_2SO_4. Filtration and concentration in vacuo and purification by silica gel flash chromatography (*n*-hexane/AcOEt = 4/1) gave 93 mg (32%) of **46** as a colorless oil: ^{1}H NMR ($CDCl_3$, 400 MHz, δ; ppm) 7.51 (2H, d, J = 7.8 Hz), 7.32 (2H, t, J = 7.6 Hz), 7.16 (1H, broad s), 7.10 (1H, t, J = 7.3 Hz), 5.41 (2H, s), 2.65 (2H, t, J = 7.3 Hz), 2.36 (2H, t, J = 7.6 Hz), 1.74 (2H, quintet, J = 7.1 Hz), 1.66 (2H, quintet, J = 7.1 Hz), 1.50−1.36 (4H, m), 1.21 (9H, s); MS (EI) *m/z*: 351 (M^+); HRMS calcd for $C_{19}H_{29}NO_3S$ 351.187, found 351.189.

Biology. Enzyme Assays. The assay of HDAC activity was performed using an HDAC fluorescent activity assay/drug discovery kit (AK-500, BIOMOL Research Laboratories). HeLa nuclear extracts (0.5 μL/well) were incubated at 37 °C with 25 μM of Fluor de Lys substrate and various concentrations of samples. Reactions were stopped after 30 min by adding Fluor de Lys Developer with trichostatin A which stops further deacetylation. Then, 15 min after addition of this developer, the fluorescence of the wells was measured on a fluorometric reader with excitation set at 360 nm and emission detection set at 460 nm, and the % inhibition was calculated from the fluorescence readings of inhibited wells relative to those of control wells. The concentration of compound which results in 50% inhibition was determined by plotting the log[Inh] versus the logit function of the % inhibition. IC_{50} values are

determined using a regression analysis of the concentration/inhibition data.

Lineweaver–Burk Double-Reciprocal Plot Analysis. The assay of HDAC activity was performed using an HDAC fluorescent activity assay/drug discovery kit (AK-500, BIOMOL Research Laboratories). HeLa nuclear extracts (0.5 μL/well) were incubated at 37 °C with Fluor de Lys substrate (50, 100, 200, or 400 μM) in the presence of 0, 0.03, 0.1, or 0.3 μM of compound **7**. Reactions were stopped after 10 min by adding Fluor de Lys Developer with trichostatin A which stops further deacetylation. Then, 15 min after addition of this developer, the fluorescence of the wells was measured on a fluorometric reader with excitation set at 360 nm and emission detection set at 460 nm.

Monolayer Growth Inhibition Assay. Cancer cells were plated in 96-well plates at initial densities of 1500 cells/well and incubated at 37 °C. After 24 h, cells were exposed to test compounds at various concentrations in 10% FBS-supplemented RPMI-1640 medium at 37 °C in 5% CO_2 for 48 h. The medium was removed and replaced with 200 μL of 0.5 mg/mL of Methylene Blue in RPMI-1640 medium, and cells were incubated at room temperature for 30 min. Supernatants were removed from the wells, and Methylene Blue dye was dissolved in 100 μL/well of 3% aqueous HCl. Absorbance was determined on a microplate reader (BioRad) at 660 nm.

Western Blot Analysis. HCT-116 cells (purchased from ATCC) (1×10^6) treated for 8 h with SAHA and compound **51** at the indicated concentrations in 10% FBS-supplemented McCoy's 5A medium were collected and sonicated. Protein concentrations of the lysates were determined by using a Bradford protein assay kit (Bio-Rad Laboratories); equivalent amounts of proteins from each lysate were resolved in 15% SDS-polyacrylamide gel and then transferred onto nitrocellulose membranes (Bio-Rad Laboratories). After blocking with Tris-buffered saline (TBS) containing 0.1% Tween 20 (TBST) containing 3% skim milk for 30 min, the transblotted membrane was incubated with hyperacetylated histone H4 antibody (Upstate Biotechnology) (1:2000) or $p21^{WAF1/CIP1}$ antibody (Medical and Biological Laboratories) (1: 200) in TBST containing 3% skim milk at 4 °C overnight. After treatment with the primary antibody, the membrane was washed twice with water for anti- hyperacetylated histone H4, or three times with TBS for anti-$p21^{WAF1/CIP1}$, then incubated with goat anti-rabbit or anti-mouse IgG-horseradish peroxidase conjugates (1:10000 or 1:5000) for 1.5 h at room temperature and washed twice with water for anti- hyperacetylated histone H4, or three times with TBS for anti-$p21^{WAF1/CIP1}$. The immunoblots were visualized by enhanced chemiluminescence.

Molecular Modeling. Docking and subsequent scoring were performed using Macromodel 8.1 software. Coordinates of HDAC8 complexed with MS344 were taken from the Brookhaven Protein Data Bank (PDB code 1T67) and hydrogen atoms were added computationally at appropriate positions. The structures of SAHA and compound **7** bound to HDAC8 were constructed by molecular mechanics (MM) energy minimization. The starting positions of SAHA and compound **7** were determined manually: the benzene ring and the linker parts were superimposed in the active site onto its crystallographic MS344 counterpart. The conformations of SAHA and compound **7** in the active site were minimized by a MM calculation based upon the OPLS-AA force field with each parameter set as follows: solvent: water, method: LBFGS, max. no. iterations: 10 000, converge on: gradient, convergence threshold: 0.05.

Acknowledgment. This work was supported in part by grants from the Health Sciences Foundation of the Ministry of Health, Labor and Welfare of Japan, and the Mochida Memorial Foundation for Medical and Pharmaceutical Research. We thank the Screening Committee of New Anticancer Agents, supported by a Grant-in-Aid for Scientific Research on Priority Area "Cancer" from the Ministry of Education, Culture, Sports, Science and Technology of Japan, for cancer cell growth inhibition assay results.

Supporting Information Available: Results of the elemental analysis of **4**–**21**, **23**–**45**, **47**, **49**–**54**, and **55** are reported. This material is available free of charge via the Internet at http://pubs.acs.org.

References

(1) (a) Grozinger, C. M.; Schreiber, S. L. Deacetylase Enzymes: Biological Functions and the Use of Small-Molecule Inhibitors. *Chem. Biol.* **2002**, *9*, 3–16. (b) Kouzarides, T. Histone acetylases and deacetylases in cell proliferation. *Curr. Opin. Genet. Dev.* **1999**, *9*, 40–48. (c) Hassig, C. A.; Schreiber, S. L. Nuclear histone acetylases and deacetylases and transcriptional regulation: HATs off to HDACs. *Curr. Opin. Chem. Biol.* **1997**, *1*, 300–308.

(2) Taunton, J.; Hassig, C. A.; Schreiber, S. L. A Mammalian Histone Deacetylase Related to the Yeast Transcriptional Regulator Rpd3p. *Science* **1996**, *272*, 408–411.

(3) Sambucetti, L. C.; Fischer, D. D.; Zabludoff, S.; Kwon, P. O.; Chamberlin, H. Trogani, N.; Xu, H.; Cohen, D. Histone Deacetylase Inhibition Selectively Alters the Activity and Expression of Cell Cycle Proteins Leading to Specific Chromatin Acetylation and Antiproliferative Effects. *J. Biol. Chem.* **1999**, *274*, 34940–34947.

(4) (a) Yoshida, M.; Horinouchi, S.; Beppu, T.Trichostatin A and trapoxin: Novel chemical probes for the role of histone acetylation in chromatin structure and function. *BioEssays* **1995**, *17*, 423–430. (b) Richon, V. M.; Webb, Y.; Merger, R.; Sheppard, T.; Jursic, B.; Ngo, L.; Civoli, F.; Breslow, R.; Rifkind, R. A.; Marks, P. A. Second generation hybrid polar compounds are potent inducers of transformed cell differentiation. *Proc. Natl. Acad. Sci. U.S.A.* **1996**, *93*, 5705–5708. (c) Richon, V. M.; Emiliani, S.; Verdin, E.; Webb, Y.; Breslow, R.; Rifkind, R. A.; Marks, P. A. A class of hybrid polar inducers of transformed cell differentiation inhibits histone deacetylases. *Proc. Natl. Acad. Sci. U.S.A.* **1998**, *95*, 3003–3007.

(5) Cohen, L. A.; Amin, S.; Marks, P. A.; Rifkind, R. A.; Desai, D.; Richon, V. M. Chemoprevention of carcinogen-induced mammary tumorigenesis by the hybrid polar cytodifferentiation agent, suberanilohydroxamic acid (SAHA). *Anticancer Res.* **1999**, *19*, 4999–5005.

(6) (a) For a review, see: Miller, T. A.; Witter, D. J.; Belvedere, S. Histone Deacetylase Inhibitors. *J. Med. Chem.* **2003**, *46*, 5097–5116. (b) For a review, see: Yoshida, M.; Matsuyama, A.; Komatsu, Y.; Nishino, N. From discovery to the coming generation of histone deacetylase inhibitors. *Curr. Med. Chem.* **2003**, *10*, 2351–2358. (c) For a review, see: Miller, T. A. Patent status of histone deacetylase inhibitors. *Expert Opin. Ther. Pat.* **2004**, *14*, 791–804. (d) Remiszewski, S. W.; Sambucetti, L. C.; Bair, K. W.; Bontempo, J.; Cesarz, D.; Chandramouli, N.; Chen, R.; Cheung, M.; Cornell-Kennon, S.; Dean, K.; Diamantidis, G.; France, D.; Green, M. A.; Howell, K. L.; Kashi, R.; Kwon, P.; Lassota, P.; Martin, M. S.; Mou, Y.; Perez, L. B.; Sharma, S.; Smith, T.; Sorensen, E.; Taplin, F.; Trogani, N.; Versace, R.; Walker, H.; Weltchek-Engler, S.; Wood, A.; Wu, A.; Atadja, P. *N*-Hydroxy-3-phenyl-2-propenamides as Novel Inhibitors of Human Histone Deacetylase with in Vivo Antitumor Activity: Discovery of (2*E*)-*N*-Hydroxy-3-[4-[[(2-hydroxyethyl)[2-(1*H*-indol-3-yl)ethyl]amino]methyl]phenyl]-2-propenamide (NVP-LAQ824). *J. Med. Chem.* **2003**, *46*, 4609–4624. (e) Kim, D.-K. Lee, J. Y.; Kim, J.-S.; Ryu, J.-H.; Choi, J.-Y.; Lee, J. W.; Im, G.-J.; Kim, T.-K.; Seo, J. W.; Park, H.-J.; Yoo, J.; Park, J.-H.; Kim, T.-Y.; Bang, Y.-J. Synthesis and Biological Evaluation of 3-(4-Substituted-phenyl)-*N*-hydroxy-2-propenamides, a New Class of Histone Deacetylase Inhibitors. *J. Med. Chem.* **2003**, *46*, 5745–5751. (f) Lu, Q.; Yang, Y.-T.; Chen, C.-S.; Davis, M.; Byrd, J. C.; Etherton, M. R.; Umar, A.; Chen, C.-S. Zn^{2+}-Chelating, Motif-Tethered, Short-Chain Fatty Acids as a Novel Class of Histone Deacetylase Inhibitors. *J. Med. Chem.* **2004**, *47*, 467–474. (g) Mai, A.; Massa, S.; Cerbara, I.; Valente, S.; Ragno, R.; Bottoni, P.; Scatena, R.; Loidl, P.; Brosch, G. 3-(4-Aroyl-1-methyl-1*H*-2-pyrrolyl)-*N*-hydroxy-2-propenamides as a New Class of Synthetic Histone Deacetylase Inhibitors. 2. Effect of Pyrrole-C_2 and/or $-C_4$ Substitutions on Biological Activity. *J. Med. Chem.* **2004**, *47*, 1098–1109. (h) Ragno, R.; Mai, A.; Massa, S.; Cerbara, I.; Valente, S.; Bottoni, P.; Scatena, R.; Jesacher, F.; Loidl, P.; Brosch, G. 3-(4-Aroyl-1-methyl-1*H*-pyrrol-2-yl)-*N*-hydroxy-2-propenamides as a New Class of Synthetic Histone Deacetylase Inhibitors. 3. Discovery of Novel Lead Compounds through Structure-Based Drug Design and Docking Studies. *J. Med. Chem.* **2004**, *47*, 1351–1359. (i) Glenn, M. P.; Kahnberg, P.; Boyle, G. M.; Hansford, K. A.; Hans, D.; Martyn, A. C.; Parsons, P. G.; Fairlie, D. P. Antiproliferative and Phenotype-Transforming Antitumor Agents Derived from Cysteine. *J. Med. Chem.* **2004**, *47*, 2984–2994.

(7) (a) Finnin, M. S.; Donigian, J. R.; Cohen, A.; Richon, V. M.; Rifkind, R. A.; Marks, P. A.; Breslow, R.; Pavletich, N. P. Structures of a histone deacetylase homologue bound to the TSA and SAHA inhibitors. *Nature* **1999**, *401*, 188−193. (b) Somoza, J. R.; Skene, R. J.; Katz, B. A.; Mol, C.; Ho, J. D.; Jennings, A. J.; Luong, C.; Arvai, A.; Buggy, J. J.; Chi, E.; Tang, J.; Sang, B.-C.; Verner, E,; Wynands, R.; Leahy, E. M.; Dougan, D. R.; Snell, G.; Navre, M.; Knuth, M. W.; Swanson, R. V.; McRee, D. E.; Tari, L. W. Structural Snapshots of Human HDAC8 Provide Insights into the Class I Histone Deacetylases. *Structure* **2004**, *12*, 1325−1334.

(8) (a) Mulder, G. J.; Meerman, J. H. Sulfation and glucuronidation as competing pathways in the metabolism of hydroxamic acids: the role of *N,O*-sulfonation in chemical carcinogenesis of aromatic amines. *Environ. Health Perspect.* **1983**, *49*, 27−32. (b) Vassiliou, S.; Mucha, A.; Cuniasse, P.; Georgiadis, D.; Lucet-Levannier, K.; Beau, F.; Kannan, R.; Murphy, G.; Knaeuper, V.; Rio, M. C.; Basset, P.; Yiotakis, A.; Dive, V. Phosphinic Pseudo-Tripeptides as Potent Inhibitors of Matrix Metalloproteinases: A Structure−Activity Study. *J. Med. Chem.* **1999**, *42*, 2610−2620.

(9) (a) Wong, J. C.; Hong, R.; Schreiber, S. L. Structural Biasing Elements for In−Cell Histone Deacetylase Paralog Selectivity. *J. Am. Chem. Soc.* **2003**, *125*, 5586−5587. (b) Haggarty, S. J.; Koeller, K. M.; Wong, J. C.; Butcher, R. A.; Schreiber, S. L. Multidimensional Chemical Genetic Analysis of Diversity-Oriented Synthesis-Derived Deacetylase Inhibitors Using Cell-Based Assays. *Chem. Biol.* **2003**, *10*, 383−396.

(10) (a) Suzuki, T.; Ando, T.; Tsuchiya, K.; Fukazawa, N.; Saito, A.; Mariko, Y.; Yamashita, T.; Nakanishi, O.Synthesis and Histone Deacetylase Inhibitory Activity of New Benzamide Derivatives. *J. Med. Chem.* **1999**, *42*, 3001−3003. (b) Vaisburg, A.; Bernstein, N.; Frechette, S.; Allan, M.; Abou-Khalil, E.; Leit, S.; Moradei, O.; Bouchain, G.; Wang, J.; Woo, S. H.; Fournel, M.; Yan, P. T.; Trachy-Bourget, M.-C.; Kalita, A.; Beaulieu, C.; Li, Z.; MacLeod, A. R.; Besterman, J. M.; Delorme, D. (2-Amino-phenyl)-amides of ω-substituted alkanoic acids as new histone deacetylase inhibitors. *Bioorg. Med. Chem. Lett.* **2004**, *14*, 283−287.

(11) (a) Frey, R. R.; Wada, C. K.; Garland, R. B.; Curtin, M. L.; Michaelides, M. R.; Li, J.; Pease, L. J.; Glaser, K. B.; Marcotte, P. A.; Bouska, J. J.; Murphy, S. S.; Davidsen, S. K. Trifluoromethyl Ketones as Inhibitors of Histone Deacetylase. *Bioorg. Med. Chem. Lett.* **2002**, *12*, 3443−3447. (b) Wada, C. K.; Frey, R. R.; Ji, Z.; Curtin, M. L.; Garland, R. B.; Holms, J. H.; Li, J.; Pease, L. J.; Guo, J.; Glaser, K. B.; Marcotte, P. A.; Richardson, P. L.; Murphy, S. S.; Bouska, J. J.; Tapang, P.; Magoc, T. J.; Albert, D. H.; Davidsen, S. K.; Michaelides, M. R. α-Keto Amides as Inhibitors of Histone Deacetylase. *Bioorg. Med. Chem. Lett.* **2003**, *13*, 3331−3335. (c) Vasudevan, A.; Ji, Z.; Frey, R. R.; Wada, C. K.; Steinman, D.; Heyman, H. R.; Guo, Y.; Curtin, M. L.; Guo, J.; Li, J.; Pease, L.; Glaser, K. B.; Marcotte, P. A.; Bouska, J. J.; Davidsen, S. K.; Michaelides, M. R. Heterocyclic Ketones as Inhibitors of Histone Deacetylase. *Bioorg. Med. Chem. Lett.* **2003**, *13*, 3909−3913.

(12) Wu, T. Y. H.; Hassig, C.; Wu, Y.; Ding, S.; Schultz, P. G. Design, synthesis, and activity of HDAC inhibitors with a *N*-formyl hydroxylamine head group. *Bioorg. Med. Chem. Lett.* **2004**, *14*, 449−453.

(13) (a) Suzuki, T.; Nagano, Y.; Matsuura, A.; Kohara, A.; Ninomiya, S.; Kohda, K.; Miyata, N. Novel Histone Deacetylase Inhibitors: Design, Synthesis, Enzyme Inhibition, and Binding Mode Study of SAHA-Based Non-hydroxamates. *Bioorg. Med. Chem. Lett.* **2003**, *13*, 4321−4326. (b) Suzuki, T.; Kouketsu, A.; Matsuura, A.; Kohara, A.; Ninomiya, S.; Kohda, K.; Miyata, N. Thiol-based SAHA analogues as potent histone deacetylase inhibitors. *Bioorg. Med. Chem. Lett.* **2004**, *14*, 3313−3317.

(14) Miyaura, N.; Suzuki, A. Palladium-catalyzed cross-coupling reaction of organoboron compounds. *Chem. Rev.* **1995**, *95*, 2457−2483.

(15) Ondetti, M. A.; Rubin, B.; Cushman, D. W. Design of specific inhibitors of angiotensin-converting enzyme: new class of orally active antihypertensive agents. *Science* **1977**, *196*, 441−444.

(16) Whittaker, M.; Floyd, C. D.; Brown, P.; Gearing, A. J. H. Design and Therapeutic Application of Matrix Metalloproteinase Inhibitors. *Chem. Rev.* **1999**, *99*, 2735−2776.

(17) (a) Furumai, R.; Matsuyama, A.; Kobashi, N.; Lee, K.-H.; Nishiyama, M.; Nakajima, H.; Tanaka, A.; Komatsu, Y.; Nishino, N.; Yoshida, M.; Horinouchi, S. FK228 (Depsipeptide) as a Natural Prodrug That Inhibits Class I Histone Deacetylases. *Cancer Res.* **2002**, *62*, 4916−4921. (b) Nishino, N.; Jose, B.; Okamura, S.; Ebisusaki, S.; Kato, T.; Sumida, Y.; Yoshida, M. Cyclic Tetrapeptides Bearing a Sulfhydryl Group Potently Inhibit Histone Deacetylases. *Org. Lett.* **2003**, *5*, 5079−5082.

(18) Christianson, D. W.; Lipscomb, W. N. Carboxypeptidase A.*Acc. Chem. Res.* **1989**, *22*, 62−69.

(19) Moree, W. J.; van der Marel, G. A.; Liskamp, R. M. J.Peptides containing a sulfinamide or a sulfonamide moiety: New transition-state analogues. *Tetrahedron Lett.* **1991**, *32*, 409−412.

(20) Kijima, M.; Yoshida, M.; Sugita, K.; Horinouchi, S.; Beppu, T. Trapoxin, an antitumor cyclic tetrapeptide, is an irreversible inhibitor of mammalian histone deacetylase. *J. Biol. Chem.* **1993**, *268*, 22429−22435.

(21) Mercaptoacetamide **14** is also attractive for further study. The results will be reported soon.

(22) (a) Jung, M.; Brosch, G.; Kölle, D.; Scherf, H.; Gerhäuser, C.; Loidl, P. Amide Analogues of Trichostatin A as Inhibitors of Histone Deacetylase and Inducers of Terminal Cell Differentiation. *J. Med. Chem.* **1999**, *42*, 4669−4679. (b) Remiszewski, S. W.; Sambucetti, L. C.; Atadja, P.; Bair, K. W.; Cornell, W. D.; Green, M. A.; Howell, K. L.; Jung, M.; Kwon, P.; Trogani, N.; Walker, H. Inhibitors of Human Histone Deacetylase: Synthesis and Enzyme and Cellular Activity of Straight Chain Hydroxamates. *J. Med. Chem.* **2002**, *45*, 753−757.

(23) Gagnard, V.; Leydet, A.; Morere, A.; Montero, J.-L.; Lefebvre, I.; Gosselin, G.; Pannecouque, C.; De Clercq, E.Synthesis and in vitro evaluation of *S*-acyl-3-thiopropyl prodrugs of Foscarnet. *Bioorg. Med. Chem.* **2004**, *12*, 1393−1402.

(24) Barber, I.; Rayner, B.; Imbach, J.-L. The prooligonucleotide approach. I. Esterase-mediated reversibility of dithymidine *S*-alkyl-phosphorothioates to dithymidine phosphorothioates. *Bioorg. Med. Chem. Lett.* **1995**, *5*, 563−568.

(25) Mohamadi, F.; Richards, N. G. J.; Guida, W. C.; Liskamp, R.; Lipton, M.; Caufield, C.; Chang, G.; Hendrickson, T.; Still, W. C. MACROMODEL − an integrated software system for modeling organic and bioorganic molecules using molecular mechanics. *J. Comput. Chem.* **1990**, *11*, 440−467.

(26) Mai, A.; Esposito, M.; Sbardella, G.; Massa, S.A new facile and expeditious synthesis of *N*-hydroxy-*N'*-phenyloctanediamide, a potent inducer of terminal cytodifferentiation. *Org. Prep. Proced. Int.* **2001**, *33*, 391−394.

JM049207J

Available online at www.sciencedirect.com
SCIENCE DIRECT®
Bioorganic & Medicinal Chemistry Letters
ELSEVIER
Bioorganic & Medicinal Chemistry Letters 15 (2005) 1547–1551

Design, synthesis, and biological activity of novel PPARγ ligands based on rosiglitazone and 15d-PGJ_2

Shinya Usui, Takayoshi Suzuki, Yoshifumi Hattori, Kazuma Etoh, Hiroki Fujieda, Makoto Nishizuka, Masayoshi Imagawa, Hidehiko Nakagawa, Kohfuku Kohda† and Naoki Miyata*

Graduate School of Pharmaceutical Sciences, Nagoya City University, 3-1 Tanabe-dori, Mizuho-ku, Nagoya, Aichi 467-8603, Japan

Received 25 December 2004; revised 30 January 2005; accepted 31 January 2005

Abstract—To develop novel PPARγ ligands, we synthesized thirteen 3-{4-(2-aminoethoxy)phenyl}propanoic acid derivatives, which are designed based on the structures of rosiglitazone and 15d-PGJ_2. Among these compounds, compound **9** was found to be as potent as rosiglitazone in a binding assay and a preadipocyte differentiation test. Molecular modeling suggested that the nonyl group of **9** interacted with hydrophobic amino acid residues constructing the hydrophobic region of PPARγ protein where the alkyl chain of 15d-PGJ_2 is expected to be located.

Peroxisome proliferator-activated receptors (PPARα, PPARγ, and PPARδ) belong to the nuclear receptor superfamily and act as ligand-activated transcription factors.[1–3] These receptors play a pivotal roles in regulating the expression of a large number of genes involved in lipid metabolism and energy balance.[4] Many studies on PPARs have been performed, and these efforts led to the discovery of the clinically useful thiazolidinedione (TZD) class of insulin sensitizers such as rosiglitazone[5] and pioglitazone[6] (Fig. 1), which are potent PPARγ agonists used in the treatment of Type 2 diabetes. However, the use of TZDs has been limited because of their poor safety profiles. For example, troglitazone, which came out to the market first, disappeared from the market due to its severe hepatic toxicity in 1999,[7] and rosiglitazone is reported to be associated with liver, cardiovascular, and hematological toxicities.[8] We therefore initiated a search for non-TZD PPARγ ligands with the goal of finding novel insulin sensitizers. In this letter, we report the design, synthesis, and biological activity of non-TZD PPARγ ligands based on the structure of rosiglitazone and 15-deoxy-Δ-12,14-prostaglandin J_2 (15d-PGJ_2).

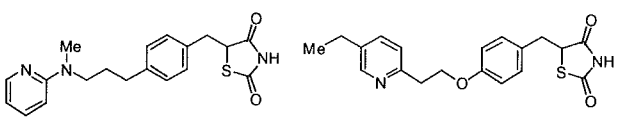

Rosiglitazone Pioglitazone

Figure 1. Structures of rosiglitazone (GSK) and pioglitazone (Takeda).

The compounds prepared for this study are shown in Figure 2, and the routes used for their synthesis are illustrated in Schemes 1–4. Scheme 1 shows the preparation of *N*-(pyridin-2-yl)-*N*-alkyl derivatives **1–3** bearing a methyl, ethyl, and propyl group, respectively, on their nitrogen atom as an alkyl chain.[9] The protection of dialkylamine **14a–c** by $(Boc)_2O$ gave **15a–c**.[10] The Mitsunobu reaction[11] was applied to the conversion of **15a–c** into 3-{4-(2-aminoethoxy)phenyl}propanoic acid derivatives **16a–c**: treatment of **15a–c** with diethylazodicarboxylate, PPh_3, and 3-(4-hydroxyphenyl)propanoic acid methyl ester **21** gave ethers **16a–c**. The *N*-Boc groups of **16a–c** were removed with trifluoroacetic acid to give amines **17a–c**. Treatment of **17a–c** with 2-fluoropyridine, or 2-chloropyridine gave *N*-(pyridin-2-yl)-*N*-alkyl compounds **18a–c** via nucleophilic aromatic substitution, and subsequent hydrolysis afforded carboxylic acids **1–3**.

Keywords: PPARγ ligand; 15d-PGJ_2; Insulin sensitizer; Agonist.
* Corresponding author. Tel./fax: +81 52 836 3407; e-mail: miyata-n@phar.nagoya-cu.ac.jp
† Current address: Faculty of Pharmaceutical Sciences, Musashino University, 1-1-20 Shin-machi, Nishi-Tokyo City, Tokyo 202-8585, Japan.

0960-894X/$ - see front matter © 2005 Elsevier Ltd. All rights reserved.
doi:10.1016/j.bmcl.2005.01.074

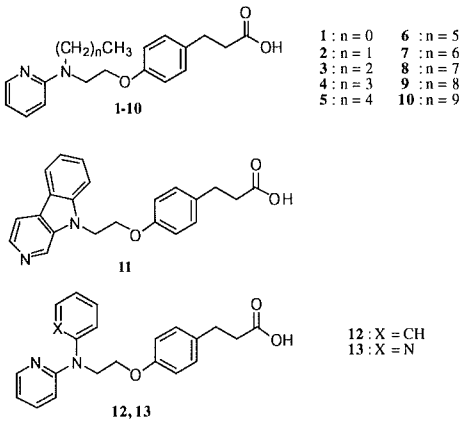

Figure 2. Structures of compounds **1**–**13**.

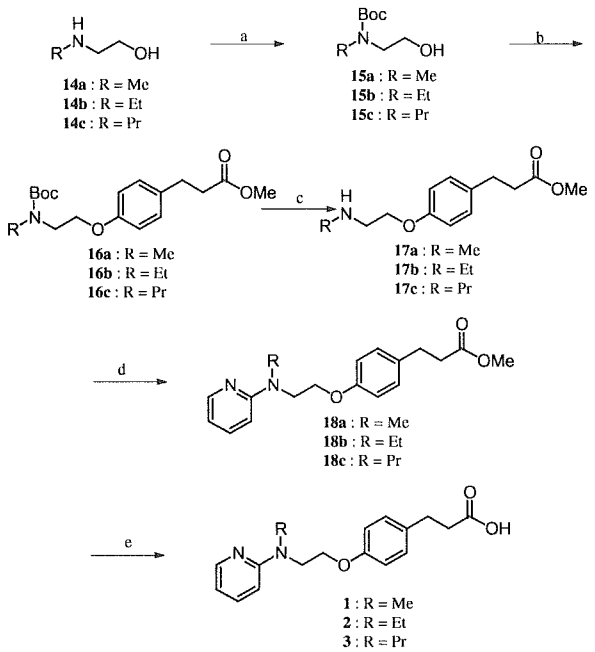

Scheme 1. Reagents and conditions: (a) Boc_2O, CH_2Cl_2, 0 °C to rt, 91–100%; (b) DEAD, PPh_3, 3-(4-hydroxyphenyl)propanoic acid methyl ester **21**, THF, 0 °C to rt, 49–63%; (c) TFA, CH_2Cl_2, 0 °C to rt, 81–94%; (d) 2-fluoropyridine or 2-chloropyridine, DMF, reflux, 7–38%; (e) aq NaOH, THF/MeOH, rt, 78–92%.

The preparation of the other *N*-(pyridin-2-yl)-*N*-alkyl derivatives **4**–**10** is outlined in Scheme 2. The preparation of 2-alkylamino pyridine **20a**–**g** was achieved by the method of Buchwald:[12] treatment of **19** with *n*-alkylamine, $Pd_2(DBA)_3$, BINAP, and *t*-BuONa in toluene under reflux. Propanoic acid methyl ester **21** was allowed to react with 1,2-dibromoethane to give ether **22**. Coupling between amines **20a**–**g** and ether **22** afforded *N*-(pyridin-2-yl)-*N*-alkyl compounds **23a**–**g**, and subsequent hydrolysis afforded carboxylic acids **4**–**10**.

N-(2-Pyridin-2-yl)-*N*-aryl derivatives **11**–**13** were prepared by the procedure outlined in Schemes 3 and 4.

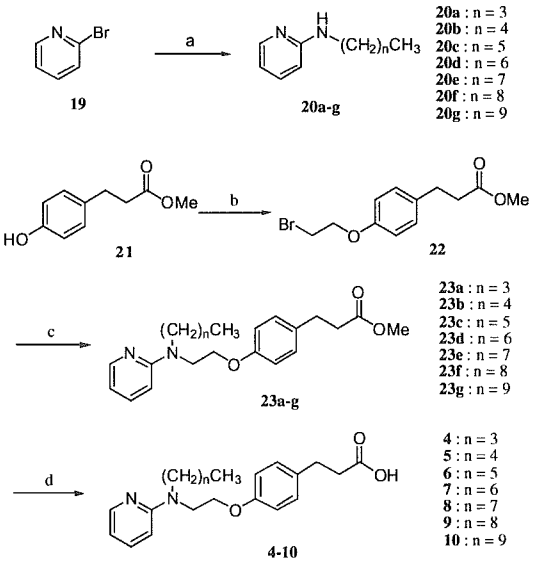

Scheme 2. Reagents and conditions: (a) $CH_3(CH_2)_nNH_2$, $Pd_2(DBA)_3$, BINAP, *t*-BuOH, toluene, 80 °C, 7–53%; (b) 1,2-dibromoethane, K_2CO_3, THF, 115 °C, 25%; (c) **20a**–**g**, Et_3N, KI, THF, 120 °C, 2–25%; (d) aq NaOH, THF, rt, 81–96%.

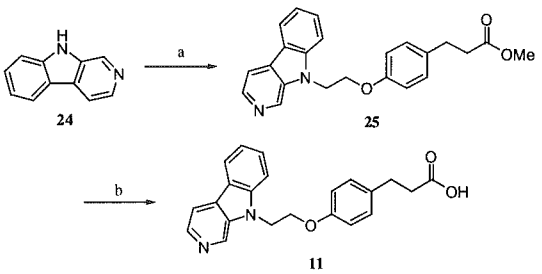

Scheme 3. Reagents and conditions: (a) (i) NaH, DMF, rt; (ii) **22**, KI, 90 °C, 72%; (b) aq NaOH, THF, rt, 89%.

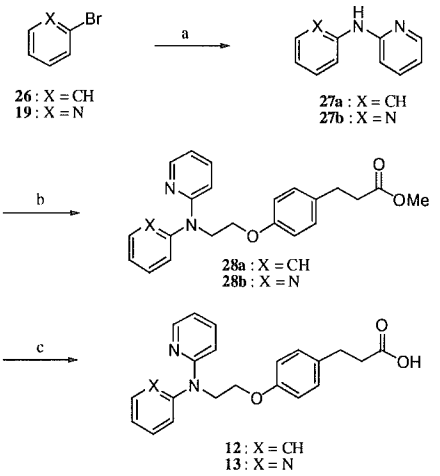

Scheme 4. Reagents and conditions: (a) 2-aminopyridine, $Pd_2(DBA)_3$, BINAP, *t*-BuONa, toluene, 80 °C, 70–88%; (b) (i) NaH, DMF, rt, (ii) **22**, KI, 90 °C, 18–30%; (c) aq NaOH, THF, rt, 70–80%.

Norharman **24** was reacted with bromide **22** in the presence of sodium hydride in DMF to give 9*H*-β-carboline compound **25**, and subsequent hydrolysis gave compound **11** (Scheme 3). Compounds **27a** and **b** were prepared in the same way as 2-alkylamino pyridines **20a–g** (Scheme 4). Compounds **27a** and **b** were allowed to react with bromide **22** in the presence of sodium hydride in DMF to give compounds **28a** and **b**. Treatment of **28a** and **b** with aqueous NaOH gave *N*-(pyridin-2-yl)-*N*-phenyl derivative **12** and dipyridinyl derivative **13**.

The binding affinity of the compounds for PPARγ was evaluated with a CoA–BAP system (Microsystems).[13] In this system, the alkaline phosphatase (AP) activity is directly proportional to the PPARγ-binding affinity of the ligands.

Since it has been revealed that the TZD ring can be replaced by a carboxyl group,[14] we initially examined the binding affinity for PPARγ of compound **1**, in which the TZD group of rosiglitazone is replaced by a carboxyl group. Although compound **1** did not show any activity at 0.1 and 1 μM, a certain level of activity was observed at 10 μM (Table 1, line 1). For the further design of PPARγ ligands, we focused on the alkyl chain of 15d-PGJ_2,[15,16] an endogenous ligand of PPARγ. Since certain fatty acids with a long alkyl chain are known to be natural PPARγ ligands,[17] the hydrophobic moiety is assumed to be critical for the binding affinity for PPARγ. Our study regarding the binding mode of 15d-PGJ_2 in PPARγ protein (PDB code 1FM6) by computer calculation (Macromodel 8.1)[18] also suggested that the alkyl chain of 15d-PGJ_2 is located in the wide hydrophobic region of the PPARγ ligand-binding cavity (Fig. 3). However, the crystal structure of a PPARγ/rosiglitazone complex[19] revealed that rosiglitazone does not have any hydrophobic groups interacting with the hydrophobic amino acid residues of PPARγ. We hypothesized that the introduction of a hydrophobic group into compound **1** may increase the affinity for PPARγ (Fig. 4). We therefore designed compounds **2–10** in which alkyl groups of various lengths were introduced at the 2-aminopyridinyl moiety of compound **1**, and evaluated their ability to bind PPARγ. It was found that the affinity of compounds **1–10** was closely related to chain length, and the most potent compounds were heptyl **7**, octyl **8**, and nonyl **9**. In addition, *N*,*N*-diaryl compounds **11–13** exhibited weak activity compared with compounds **7–9** (Table 1, lines 11–13). We next compared the binding affinity of compounds **7–9** with that of rosiglitazone at lower concentrations. As shown in Figure 5, compound **9** showed the highest activity among the three, and had only slightly less affinity for PPARγ than did rosiglitazone.

Table 1. Binding affinity for PPARγ of compounds **1–13** at 0.1, 1.0, and 10 μM.[a]

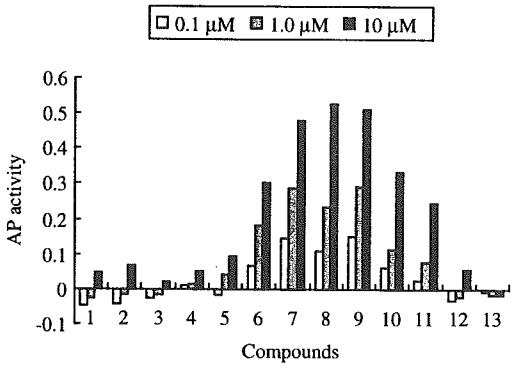

[a] Values are means of at least three experiments.

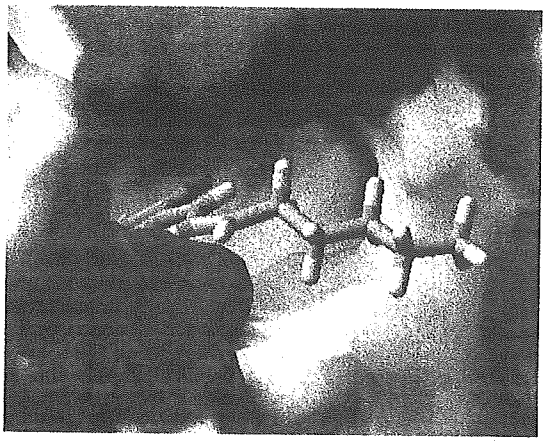

Figure 3. View of the conformation of 15d-PGJ_2 (tube) docked in PPARγ. The hydrophobic and hydrophilic regions are shown in yellow and blue, respectively.

As compound **9** was most active in our study, we used it for further evaluation. Since it has been reported that activation of PPARγ enhances adipocyte differentiation[20] and increases insulin sensitivity, compound **9** was subjected to a rat abdominal preadipocyte differentiation test.[21,22] The accumulation of neutral fat in the cells was observed after the administration of compound **9** at concentrations of 1, 2.5, and 5 μM, and the activity of compound **9** was found to be comparable to that of rosiglitazone (Fig. 6).

Since *N*-nonyl carboxylic acid **9** had a high level of activity, we studied its mode of binding to PPARγ. A low energy conformation was calculated when **9** was docked in a model based on the crystal structure of PPARγ using Macromodel 8.1 software.[18] An inspection of the simulated PPARγ/**9** complex suggested that oxygen atoms of compound **9** form hydrogen bonds with Ser 289, Tyr 327, and Tyr 473 (Fig. 7). In addition, it was shown that the nonyl group of **9** is located in the hydrophobic region formed by Phe 287, Gly 284, Ile 281, Ile 341, and Met 348 (Fig. 8) where the alkyl chain of 15d-PGJ_2 is calculated to be located (Fig. 3).

In summary, in order to explore novel PPARγ ligands, we prepared several 3-{4-(2-aminoethoxy)phenyl}propanoic acid derivatives designed based on the structures of rosiglitazone and 15d-PGJ_2. Among them, *N*-(pyridin-2-yl)-*N*-nonyl compound **9** was found to be as

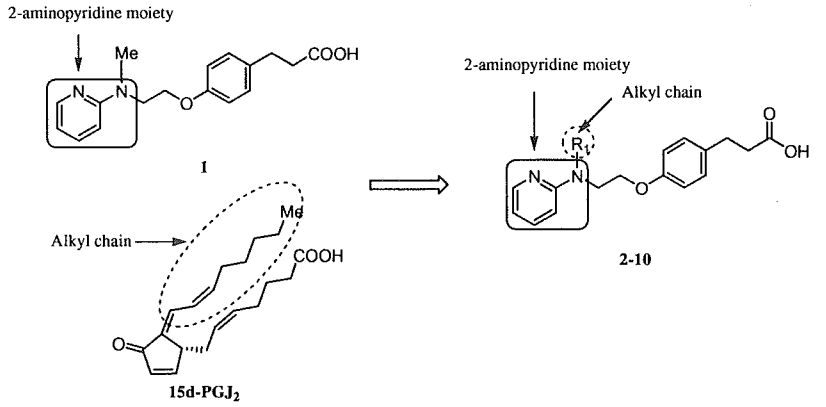

Figure 4. Structures of compounds **2–10** designed on the basis of the structure of 15d-PGJ_2 and rosiglitazone.

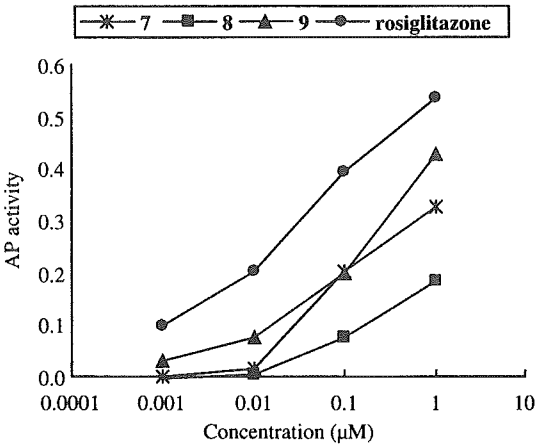

Figure 5. Binding affinity for PPARγ of rosiglitazone and compounds **7–9** at 0.001, 0.01, 0.1, and 1.0 μM. Values are means of at least three experiments.

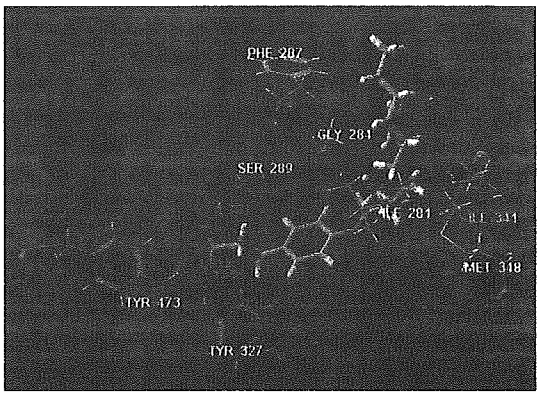

Figure 7. View of the conformation of **9** (tube) docked in PPARγ. Residues around compound **9** and hydrogen bonds are displayed as wires, and dotted lines, respectively. Figures represent distances in angstroms.

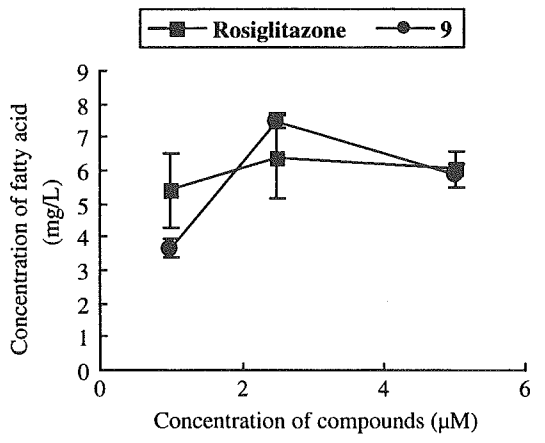

Figure 6. Accumulation of fatty acid in rat preadipocytes by rosiglitazone and compound **9**. Values are means of at least three experiments.

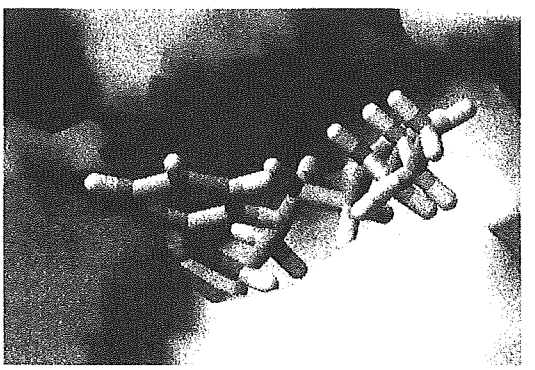

Figure 8. View of the conformation of **9** (tube) docked in PPARγ. The hydrophobic and hydrophilic regions are shown in yellow and blue, respectively.

potent as rosiglitazone in the binding assay and the preadipocyte differentiation test. Molecular modeling suggested that the carboxylate anion of **9** forms hydrogen bonds with some hydrophilic amino acid residues, and the nonyl group appropriately interacts with hydrophobic amino acid residues. The findings of this study will help provide an effective agent for Type 2 diabetes.

Currently, further detailed studies on compound **9** are under way.

Acknowledgements

This work was supported in part by grants from the Health Sciences Foundation of the Ministry of Health, Labor, and Welfare of Japan.

References and notes

1. Willson, T. M.; Brown, P. J.; Sternbach, D. D.; Henke, B. R. *J. Med. Chem.* **2000**, *43*, 527.
2. Willson, T. M.; Cobb, J. E.; Cowan, D. J.; Wiethe, R. W.; Correa, I. D.; Prakash, S. R.; Beck, K. D.; Moore, L. B.; Kliewer, S. A.; Lehmann, J. M. *J. Med. Chem.* **1996**, *39*, 665.
3. Kersten, S.; Desvergne, B.; Wahli, W. *Nature* **2000**, *405*, 421.
4. Bogacka, I.; Xie, H.; Bray, G. A.; Smith, S. R. *Diabetes Care* **2004**, *27*, 1660.
5. Cantello, B. C. C.; Cawthorone, M. A.; Cottam, G. P.; Duff, P. T.; Haigh, D.; Hindley, R. M.; Lister, C. A.; Smith, S. A.; Thurlby, P. L. *J. Med. Chem.* **1994**, *37*, 3977.
6. Momose, Y.; Meguro, K.; Ikeda, H.; Hatanaka, C.; Oi, S.; Sohda, T. *Chem. Pharm. Bull.* **1991**, *39*, 1440.
7. Liver damage warning for Troglitazone *Scrip.* **1997**, *2282*, 21.
8. Patel, J.; Miller, E.; Hu, J.; Granett, J. Diabetes **1997**, *46* (Suppl. 1), Abstr. 0578.
9. Henke, B. R.; Blanchard, S. G.; Brackeen, M. F.; Brown, K. K.; Cobb, J. E.; Collins, J. L.; Harrington, W. W.; Hashim, M. A.; Hull-Ryde, E. A.; Kaldor, I.; Kliewer, S. A.; Lake, D. H.; Leesenitzer, L. M.; Lehmann, J. M.; Lenhard, J. M.; Orband-Miller, L. A.; Miller, J. F.; Mook, R. A.; Noble, S. A.; Oliver, W.; Parks, D. J.; Plunket, K. D.; Szewczyk, J. R.; Willson, T. M. *J. Med. Chem.* **1998**, *41*, 5020.
10. Krapcho, A. P.; Maresch, M. J.; Lunn, J. *Synth. Commun.* **1993**, *23*, 2443.
11. For a review see: Mitsunobu, O. *Synthesis* **1981**, 1.
12. Wagaw, S.; Buchwald, S. L. *J. Org. Chem.* **1996**, *61*, 7240.
13. Kanayama, T.; Mamiya, S.; Nishihara, T.; Nishikawa, J. *J. Biochem.* **2003**, *133*, 791.
14. Rybczynski, P. J.; Zeck, R. E.; Dudash, J., Jr.; Combs, D. W.; Burris, T. P.; Yang, M.; Osborne, M. C.; Chen, X.; Demarest, K. T. *J. Med. Chem.* **2004**, *47*, 196.
15. Forman, B. M.; Tontonoz, P.; Chen, J.; Brun, R. P.; Spiegelman, B. M.; Evans, R. M. *Cell* **1995**, *83*, 803.
16. Kliewer, S. A.; Lenhard, J. M.; Willson, T. M.; Patel, I.; Morris, D. C.; Lehmann, J. M. *Cell* **1995**, *83*, 813.
17. Kliewer, S. A.; Umesono, K.; Noonan, D. J.; Heyman, R. A.; Evans, R. M. *Nature* **1992**, *358*, 771.
18. Docking and subsequent scoring were performed using Macromodel 8.1 software. Coordinates of PPARγ complexed with rosiglitazone were taken from the Brookhaven Protein Data Bank (PDB code 1FM6) and hydrogen atoms were added computationally at appropriate positions. The structure of a ligand bound to PPARγ was constructed by molecular mechanics (MM) energy minimization. The starting position of a ligand was determined manually: its carboxyl group was superimposed onto the TZD ring of crystallographic rosiglitazone. The conformation of the ligand in the active site was minimized by a MM calculation based upon the OPLS-AA force field with each parameter set as follows; solvent: water, method: LBFGS, Max # Iterations: 10,000, converge on: gradient, convergence threshold: 0.05.
19. Gampe, R. T., Jr.; Montana, V. G.; Lambert, M. H.; Miller, A. B.; Bledsoe, R. K.; Milburn, M. V.; Kliewer, S. A.; Willson, T. M.; Xu, H. E. *Mol. Cell* **2000**, *5*, 545.
20. Henke, B. R. *J. Med. Chem.* **2004**, *47*, 4118.
21. Lagace, D. C.; Nachtigal, M. W. *J. Biol. Chem.* **2004**, *278*, 18851.
22. In rat preadipocyte differentiation experiments, we basically followed the protocol of the preadipocyte Total Kit (TOYOBO. Co., Ltd, Osaka, Japan). Rat preadipocytes obtained from the abdominal tissue (Wistar, male, 8 weeks old) were cultured for 10 days in a humidified incubator at 37 °C and 5% CO_2 in a preadipocyte growth medium. The medium was renewed every other day. After the preadipocytes reached confluence, they were treated with preadipocyte differentiation medium containing compound **9** or rosiglitazone. The cells were cultured for 15 days with the differentiation medium renewed every three days. Accumulating neutral fat in the cells was measured as absorbance at 590 nm with a 1420 ARVO^{TM} multilabel-counter (PerkinElmer, Boston, MA, U.S.A.) after staining with lipidos liquid (TOYOBO. Co., Ltd, Osaka, Japan).

Available online at www.sciencedirect.com
SCIENCE DIRECT®
Bioorganic & Medicinal Chemistry Letters
ELSEVIER
Bioorganic & Medicinal Chemistry Letters 15 (2005) 331–335

Identification of a potent non-hydroxamate histone deacetylase inhibitor by mechanism-based drug design

Takayoshi Suzuki,* Azusa Matsuura, Akiyasu Kouketsu, Hidehiko Nakagawa and Naoki Miyata*

Graduate School of Pharmaceutical Sciences, Nagoya City University, 3-1 Tanabe-dori, Mizuho-ku, Nagoya, Aichi 467-8603, Japan

Received 10 September 2004; revised 25 October 2004; accepted 25 October 2004
Available online 13 November 2004

Abstract—In order to find novel non-hydroxamate histone deacetylase (HDAC) inhibitors, we synthesized several suberoylanilide hydroxamic acid (SAHA)-based compounds designed on the basis of the catalytic mechanism of HDACs. Among these compounds, **5b** was found to be as potent as SAHA. Kinetic enzyme assays and molecular modeling suggested that the mercaptoacetamide moiety of **5b** interacts with the zinc in the active site of HDACs and removes a water molecule from the reactive site of the deacetylation.

Histone deacetylases (HDACs) catalyze the deacetylation of the acetylated ε-amino groups of specific histone lysine residues,[1,2] and are involved in the expression of a number of genes.[3] In addition, HDACs have also been implicated in certain disease states such as cancer.[4–7] For this reason, there is a growing interest in the generation of potent small-molecule inhibitors of HDACs. Thus far, several classes of small-molecule HDAC inhibitors have been recognized.[8] Most of these are hydroxamic acid derivatives, typified by suberoylanilide hydroxamic acid (SAHA) (Fig. 3), and are thought to chelate the zinc ion in the active site.[9,10] Although hydroxamic acids are responsible for various potent inhibitors, they generally have many problems associated with their use such as low oral availability, poor in vivo stability, and undesirable side effects.[11,12] Thus, it has become increasingly desirable to find replacement groups that possess strong inhibitory action against HDACs. We and other groups have searched for a suitable hydroxamic acid replacement for HDAC inhibitors by structure-based drug design (SBDD)[13–15] ever since the crystal structure of an archaebacterial HDAC homologue (HDAC-like protein, HDLP)/SAHA complex was first reported.[9] However, SBDD has not yet led to the discovery of potent non-hydroxamate HDAC inhibitors, and the non-hydroxamates found with SBDD are approximately 10–1000-fold less potent than their corresponding hydroxamates. We therefore decided to search for hydroxamic acid replacements by an alternative approach, namely, mechanism-based drug design. In this paper, we report the mechanism-based design, synthesis, enzyme inhibition, and binding mode of non-hydroxamate HDAC inhibitors.

The crystal structures of the HDLP/hydroxamates and HDAC8/hydroxamates complexes have led to a solid understanding of not only the three dimensional structure of the active site of HDACs but also the catalytic mechanism for the deacetylation of acetylated lysine substrate.[9,10] It is proposed that the carbonyl oxygen of this substrate could bind the zinc, and the carbonyl could be attacked by a zinc-chelating water molecule (Fig. 2a), which would result in the production of deacetylated lysine via a tetrahedral carbon-containing transition state (Fig. 1a). On the basis of the proposed catalytic mechanism, we attempted to design non-hydroxamate HDAC inhibitors. First, we designed transition-state (TS) analogues. The TS of HDAC deacetylation was estimated to include a tetrahedral carbon (Fig. 1a) as with other zinc proteases.[16] To date, there has been only one report on TS analogue inhibitors of HDACs, namely, phosphorus-based SAHA analogues.[17] However, these analogues have a potency about 1000-fold less than that of SAHA. We focused attention on sulfone derivative TS analogues because it has been suggested that the sulfonamide moiety has strong similarity with the TS of amide bond hydrolysis,

Keywords: Histone deacetylase inhibitor; Non-hydroxamate.
* Corresponding authors. Tel./fax: +81 52 836 3407; e-mail addresses: suzuki@phar.nagoya-cu.ac.jp; miyata-n@phar.nagoya-cu.ac.jp

0960-894X/$ - see front matter © 2004 Elsevier Ltd. All rights reserved.
doi:10.1016/j.bmcl.2004.10.074

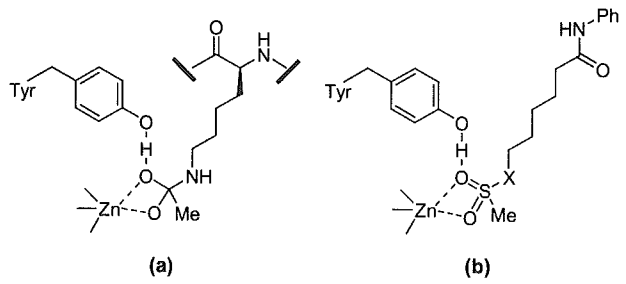

Figure 1. The transition state proposed for HDACs (a), and models for the binding of sulfone derivatives (b).

both from a steric and an electronic point of view.[18] Compounds **1** and **2**, in which a hydroxamic acid of SAHA was replaced by a sulfonamide and a sulfone, respectively, were designed as TS analogues (Figs. 1b, and 3). Our second approach was based on the proposed deacetylation mechanism whereby a zinc-chelating water molecule activated by His142 and His143 (HDAC8 numbering) makes a nucleophilic attack on the carbonyl carbon of acetylated lysine substrate (Fig. 2a). With this mechanism, if the water molecule is forcibly removed from the zinc ion, the HDACs would supposedly be inhibited. We then designed hetero atom containing substrate analogues **3**–**5** (Fig. 3). These analogues would be recognized as substrates by HDACs and would be easily taken into the active site where they could force the water molecule off the zinc ion and the reactive site of the deacetylation by chelation of the hetero atom to the zinc ion, and might behave as HDAC inhibitors (Fig. 2b).

The compounds prepared for this study are shown in Table 1. The routes used for synthesis of the compounds are indicated in Schemes 1–3. Scheme 1 shows the preparation of sulfonamide **1**, a TS analogue. The condensation of dicarboxylic acids **8a–c** with an equivalent amount of aniline gave mono-anilides **9a–c**. Carboxylic

Table 1. HDAC inhibition data for SAHA, SAHA-based transition state analogues, and substrate analogues[a]

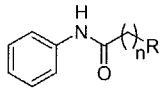

Compd	R	*n*	% Inhbtn at 100 μM	IC_{50} (μM)
SAHA[b]	–CONHOH	6	100	0.28
1	$-NHSO_2Me$	5	10	7500
2	$-SO_2Me$	6	33	230
3	$-NHCOCH_2NH_2$	5	6	>100
4	$-NHCOCH_2OH$	5	0	>100
5a	$-NHCOCH_2SH$	6	96	3.0
5b	$-NHCOCH_2SH$	5	99	0.39
5c	$-NHCOCH_2SH$	4	88	11
6	$-NHCOCH_2SAc$	5	72	22
7	$-NHCOCH_2CH_2SH$	5	78	24

[a] Values are means of at least three experiments.
[b] Prepared as described in Ref. 25.

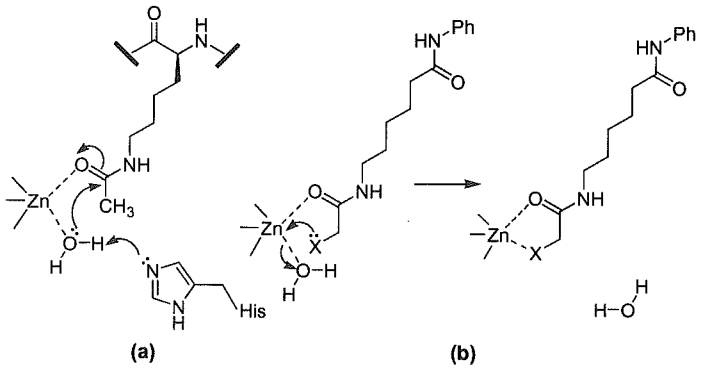

Figure 2. The mechanism proposed for the deacetylation of acetylated lysine substrate (a), and a model for the binding of hetero atom containing substrate analogues to zinc ion (b).

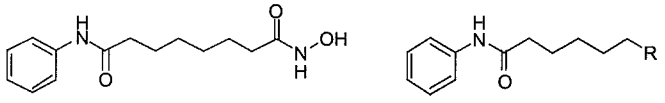

SAHA

1: R = $-NHSO_2Me$
2: R = $-CH_2SO_2Me$
3: R = $-NHCOCH_2NH_2$
4: R = $-NHCOCH_2OH$
5: R = $-NHCOCH_2SH$

Figure 3. Structures of SAHA, SAHA-based transition state analogues **1** and **2**, and hetero atom containing substrate analogues **3**–**5** designed on the basis of the deacetylation mechanism.

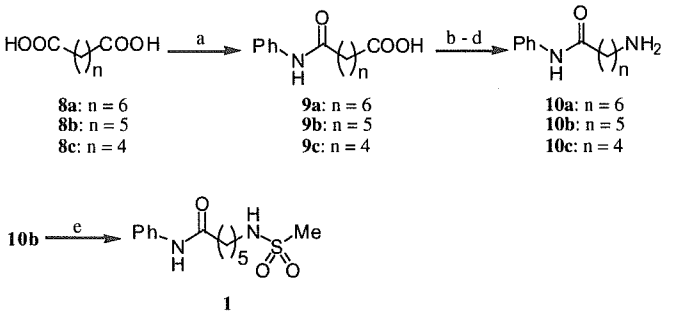

Scheme 1. Reagents and conditions: (a) aniline, 180 °C, 46–54%; (b) diphenylphosphoryl azide, Et_3N, benzene, reflux; (c) BnOH, reflux, 63–94% (two steps); (d) H_2, 5% Pd–C, MeOH, rt, 72–96%; (e) MsCl, pyridine, rt, 71%.

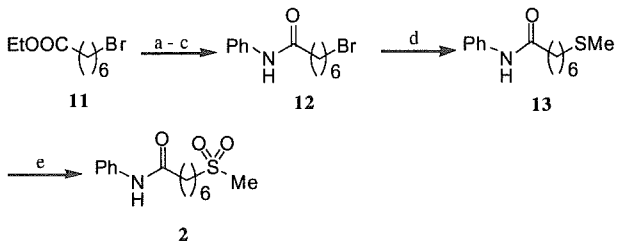

Scheme 2. Reagents and conditions: (a) $LiOH \cdot H_2O$, THF, EtOH, H_2O, rt, 99%; (b) $(COCl)_2$, DMF, CH_2Cl_2, rt; (c) aniline, Et_3N, CH_2Cl_2, rt, 87%; (d) 15% aq NaSMe, EtOH, rt, 99%; (e) *m*-chloroperoxybenzoic acid, CH_2Cl_2, rt, 70%.

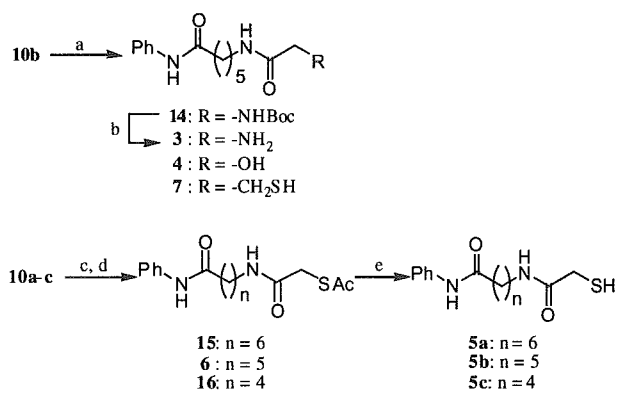

Scheme 3. Reagents and conditions: (a) RCH_2COOH, EDCI, HOBt, DMF, rt, 35–99%; (b) trifluoroacetic acid, CH_2Cl_2, rt, 84%; (c) bromoacetyl chloride, Et_3N, CH_2Cl_2, rt, 23–56%; (d) AcSK, EtOH, rt, 50–89%; (e) K_2CO_3, MeOH, rt, 28–75%.

acids **9a–c** were converted to amines **10a–c** in three steps: Curtius rearrangement of carboxylic acids **9a–c**, treatment of the resulting isocyanates with benzyl alcohol, and cleavage of the *Z* group by hydrogenolysis. Coupling between amine **10b** and methanesulfonyl chloride afforded sulfonamide **1**. Preparation of **2**, the other TS analogue, is shown in Scheme 2. 7-Bromoheptanoic acid ethyl ester **11** was converted to **12** in three steps by hydrolysis of the ester of **11**, acid chloride formation by oxalyl chloride, and condensation with aniline. Bromide **12** was allowed to react with sodium methanethiolate to give sulfide **13**, after which treatment with two equivalents of *m*-chloroperoxybenzoic acid gave sulfone **2**. Hetero atom containing substrate analogues **3–7** were prepared from amines **10** obtained above by the procedure outlined in Scheme 3. The amine **10b** was reacted with an appropriate carboxylic acid in the presence of EDCI and HOBt in DMF to give compounds **4**, **7** and **14**. The *N*-Boc group of compound **14** was removed by treating with trifluoroacetic acid to give aminoacetamide **3**. Coupling between amines **10a–c** and bromoacetyl chloride and subsequent treatment with potassium thioacetate afforded compounds **6**, **15**, and **16** and the deacetylation of these compounds in the presence of K_2CO_3 in MeOH gave mercaptoacetamides **5a–c**.

The compounds prepared for this study were evaluated using an HDAC enzyme inhibition assay[19] (Table 1). In the case of TS analogues, sulfone **2** showed anti-HDAC activity and the IC_{50} value was 230 μM, which was greater than those of phosphorus-based SAHA analogues.[17] However, sulfone **2** was approximately 820-fold less effective than SAHA. Next, we examined hetero atom containing substrate analogues. While **3** and **4** did not possess HDAC inhibitory activities,[20] potent inhibition was observed with mercaptoacetamide **5b**. Compound **5b** exhibited an IC_{50} of 0.39 μM, and its activity largely surpassed those of phosphorus compounds[17] and was comparable to those of SAHA and previously reported non-hydroxamates.[21,22] The potency of mercaptoacetamide **5a–c** was directly related to chain length, and the most potent compound was **5b**, where $n = 5$. As expected, thiol transformation into thioacetate (**6**) led to a 55-fold less potent inhibitor. This result suggests that thiolate anion generated under physiological conditions has an intimate involvement in the interaction with the zinc ion in the active site. The conversion of mercaptoacetamide to mercaptopropionamide (**7**) reduced potency as compared to compound **5b**.

Next, we studied the inhibition mechanism of mercaptoacetamide **5b**. Although the mercaptoacetamide group of **5b** was designed to make use of its chelation of the zinc ion in the active site, there is a possibility that mercaptoacetamide **5b** inhibits HDACs by forming a covalent disulfide bond with cysteine residues of these enzymes. We examined this possibility using a Lineweaver–Burk plot (a double reciprocal plot of $1/V$ versus 1/[substrate] at varying concentrations of inhibitor **5b**)

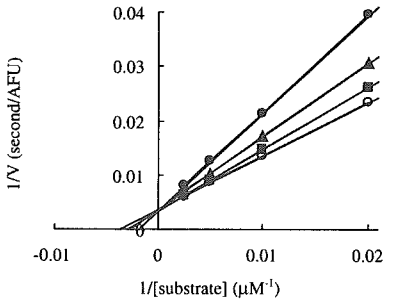

Figure 4. Reciprocal rate versus reciprocal acetyl lysine substrate concentration in the presence of 1 (●), 0.3 (▲), 0.1 (■), and 0 (○) μM of **5b**.

(Fig. 4), and the data from this study established that mercaptoacetamide **5b** engages in competitive inhibition versus acetylated lysine substrate, with an inhibition constant (K_i) of 0.78 μM. Since cysteine is not a component in the construction of the active site of HDACs, the mercaptoacetamide group of **5b** likely interacts with the zinc in the active site.

Since mercaptoacetamide **5b** was proven to act in the HDAC active center, we studied its binding mode in this site. The low energy conformation of **5b** was calculated when docked in the model based on the crystal structure of HDAC8 (PDB code 1T64, 1T67, 1T69, and 1VKG) using Macromodel 8.1 software. An inspection of the HDAC8/**5b** complex showed that the sulfur atom and oxygen atom of **5b** were located 2.44 Å and 2.04 Å from the zinc ion, respectively, and that a water molecule, which is required for the deacetylation of acetylated lysine substrate, was positioned 4.95 Å apart from the zinc ion (Fig. 5). This calculation suggests that **5b** inhibits HDACs by chelating the zinc ion in a bidentate fashion through its sulfur and oxygen atoms, and by removing a water molecule from the zinc and the reactive site of the deacetylation, without being hydrolyzed by HDACs.

In summary, in order to find novel non-hydroxamate HDAC inhibitors, we prepared several SAHA-based compounds whose designs were based on the proposed HDAC catalytic mechanism. Although transition state analogues were weakly active against HDACs, mercaptoacetamide **5b**, one of the hetero atom containing substrate analogues, was found to be as potent as SAHA. Mercaptoacetamide **5b** exhibits strong competitive inhibition versus acetylated lysine substrate. As far as we could determine, this is the first report of HDAC inhibitors with mercaptoacetamide. Since mercaptoacetamides are reported as potent, long-lived, and low-toxic matrix metalloproteinase inhibitors,[23,24] we believe that our findings in this study will provide the basis for the development of ideal HDAC inhibitors free of the problems associated with hydroxamates. Further detailed structure–activity relationship studies are currently under way and the next stage of evaluations pertaining to mercaptoacetamides **5** has begun.

Acknowledgements

This work was supported in part by grants from the Health Sciences Foundation of the Ministry of Health, Labor and Welfare of Japan, and the Mochida Memorial Foundation for Medical and Pharmaceutical Research.

References and notes

1. Grozinger, C. M.; Schreiber, S. L. *Chem. Biol.* **2002**, *9*, 3.
2. Hassig, C. A.; Schreiber, S. L. *Curr. Opin. Chem. Biol.* **1997**, *1*, 300.
3. Taunton, J.; Hassig, C. A.; Schreiber, S. L. *Science* **1996**, *272*, 408.
4. Yoshida, M.; Horinouchi, S.; Beppu, T. *BioEssays* **1995**, *17*, 423.

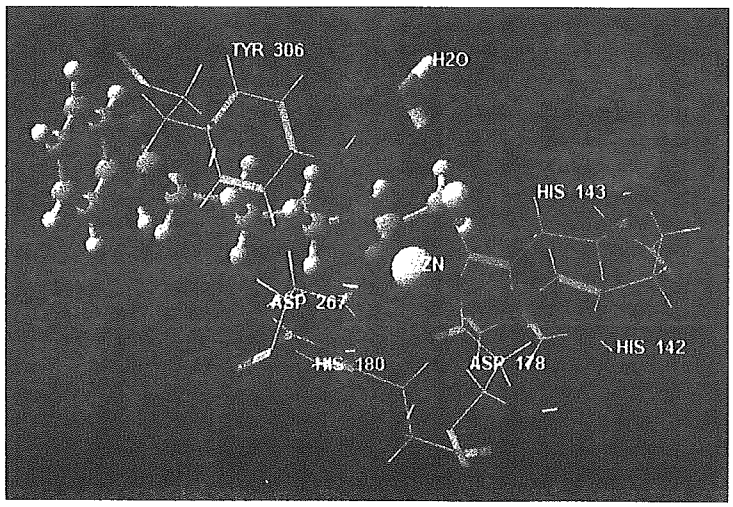

Figure 5. View of the conformation of **5b** (ball and stick) docked in the HDAC8 catalytic core. Residues around the zinc ion and a water molecule are displayed as wires and tubes, respectively.